AD-A 010 457

COATING SCIENCE AND TECHNOLOGY

B. E. KNOX, ET AL

PENNSYLVANIA STATE UNIVERSITY

PREPARED FOR:

AIR FORCE CAMBRIDGE RESEARCH LABORATORIES

DEFENSE ADVANCED RESEARCH PROJECTS AGENCY

31 JANUARY 1975

AFCRL-TR-75-0152

COATING SCIENCE AND TECHNOLOGY

B.E. Knox
K. Vedam

Materials Research Laboratory
Pennsylvania State University
University Park, Pennsylvania 16802

31 January 1975

Final Report for Period 25 April 1973 - 31 December 1974

Approved for public release; distribution unlimited

Sponsored by

Defense Advanced Research Projects Agency
ARPA Order No. 2415

Monitored by

AIR FORCE CAMBRIDGE RESEARCH LABORATORIES
AIR FORCE SYSTEMS COMMAND
UNITED STATES AIR FORCE
HANSCOM AFB, MASSACHUSETTS 01731

Unclassified

SECURITY CLASSIFICATION OF THIS PAGE (When Data Entered)

REPORT DOCUMENTATION PAGE		READ INSTRUCTIONS BEFORE COMPLETING FORM
1. REPORT NUMBER: AFCRL-TR-75-0152	2. GOVT ACCESSION NO.	3. RECIPIENT'S CATALOG NUMBER: AD-A010 457
4. TITLE (and Subtitle): COATING SCIENCE AND TECHNOLOGY		5. TYPE OF REPORT & PERIOD COVERED: Final Report 25 April 1973-31 Dec 1974
		6. PERFORMING ORG. REPORT NUMBER
7. AUTHOR(s): B. E. Knox, K. Vedam		8. CONTRACT OR GRANT NUMBER(s): F19628-73-C-0219
9. PERFORMING ORGANIZATION NAME AND ADDRESS: Materials Research Laboratory, Pennsylvania State University, University Park, Pennsylvania 16802		10. PROGRAM ELEMENT, PROJECT, TASK AREA & WORK UNIT NUMBERS: 61102E, 2415, T&WU n/a
11. CONTROLLING OFFICE NAME AND ADDRESS: Air Force Cambridge Research Laboratories, Hanscom AFB, Massachusetts 01731, Contract Monitor: Joseph J. Comer/LQO		12. REPORT DATE: 31 January 1975
		13. NUMBER OF PAGES: 56
14. MONITORING AGENCY NAME & ADDRESS (if different from Controlling Office)		15. SECURITY CLASS. (of this report): Unclassified
		15a. DECLASSIFICATION/DOWNGRADING SCHEDULE

16. DISTRIBUTION STATEMENT (of this Report)

Approved for public release; distribution unlimited

17. DISTRIBUTION STATEMENT (of the abstract entered in Block 20, if different from Report)

18. SUPPLEMENTARY NOTES **PRICES SUBJECT TO CHANGE**

This research was supported by the Defense Advanced Research Projects Agency. ARPA Order No. 2415

19. KEY WORDS (Continue on reverse side if necessary and identify by block number) Potassium chloride, zinc selenide, germanium, cadmium telluride, tetrahedral carbon, germanium oxidation, sputter-deposited films, durability testing, chemical vapor deposition, plasma polymerization, stress optic coefficients, ellipsometry, Auger electron spectroscopy, ion scattering spectrometry, electron microscopy, scanning electron microscopy, electron microprobe, IR spectroscopy, laser Raman spectroscopy

20. ABSTRACT (Continue on reverse side if necessary and identify by block number) An extensive study of the sputter-deposition of germanium films on KCl substrates was conducted. Utilizing the technique of welding the KCl substrates to the heat sink in the sputtering system has allowed us to extend the range of sputtering conditions under which germanium films can be made.

The oxidation of sputter-deposited amorphous germanium films was studied because of the possible absorption problem at 10.6 μm. Infrared spectroscopy was used to determine that the kinetics of the film oxidation followed a logarithmic rate. Ion scattering spectroscopy was used to study the composition

DD FORM 1 JAN 73 1473 EDITION OF 1 NOV 65 IS OBSOLETE S/N 0102-014-6601

Unclassified

SECURITY CLASSIFICATION OF THIS PAGE (When Data Entered)

profiles through germanium films and to show that the oxygen is uniformly distributed throughout the entire film, even penetrating into the bulk substrate for some distance. The composition profiles showed a distinct interface covering a region about 100Å thick. Thus, bulk oxidation of the germanium film occurs, even after a short exposure to air.

Preliminary studies of the sputter-deposition of CdTe on KCl were undertaken. As in the case of Ge films the nature of the sputtered CdTe film is found to be strongly dependent on the sputtering conditions. Either crystalline (cubic and/or hexagonal) or amorphous films of CdTe can be produced by controlling the Ar pressure, r.f. voltage and power and the physical geometry of the sputtering target, substrate, etc., which also affect the adherence of the film to the substrate. Ion scattering and Auger electron spectroscopy studies on sputtered CdTe films revealed that the surfaces of the films were rich in tellurium, and that small amounts of oxygen were incorporated in the film.

A method of determining the "durability" of a film on a particular substrate has been established. This involves: (a) "Scratch-test" adhesion measurements, with the critical loads normalized to the substrate hardness; (b) abrasion test measurements; (c) an evaluation of the stress conditions of the film; and (d) analysis of the interface region between the film and the substrate by compositional profiling with ion scattering and Auger electron spectroscopy. Initial results for Ge on KCl indicate that bonding between the film and the substrate is due to van der Waals forces and not to the chemical nature of the surface.

A number of cutting and polishing techniques were investigated for KCl substrates and the specimens examined with ellipsometry, a tool used extensively in the studies of both substrate surfaces and films. The degree of damage and the thickness of the damaged layers on substrate surfaces prepared for sputtering were measured to correlate different preparation techniques with certain aspects of deposition and adhesion. Electron microprobe analyses and scanning electron microscopy have been utilized widely in the initial preparatory studies.

A study of the factors involving stress in films has been made. Two types of stress may occur, thermal and intrinsic, and a stress may either be compressive or tensile. By tailoring the sputtering conditions we can prepare films of germanium on KCl which are either compressive or tensile to compensate for an expected thermal tensile stress with an intrinsic compressive stress.

Attempts to prepare germanium films on KCl substrates using chemical vapor deposition techniques were not very successful. Under the prevailing reaction conditions, the iodine utilized to transport the germanium to the deposition site (as GeI_2 and GeI_4) tended to react with the substrate surface, replacing the chlorine and etching the surface. Computer studies of the system thermodynamics showed that no parameters could be changed to enhance the deposition of germanium before the substrate was etched.

Efforts to prepare tetrahedral carbon (the so-called "diamond film") by the laser evaporation of graphite with subsequent microwave excitation of the C_3 and C_1 species were not successful. Deposition of carbon films by laser evaporation alone were successful, though the films so obtained appeared to be amorphous. However, power densities high enough to produce free jet vaporization could not be obtained with the laser system available in this laboratory.

Organic films were prepared by the plasma-polymerization technique using microwave (rather than r.f.) excitation to provide a homogeneous, pinhole-free encapsulation for optical components for environmental protection. A series of films were prepared to find the optimum deposition parameters and examined optically by scanning electron microscopy and electron microscopy to check their homogeneity.

The stress-optic coefficient of zinc selenide at 10.6 μm was measured. At this wavelength C_λ = -11.9 Brewsters; the piezo-optic coefficient, $q_{11} - q_{12}$ = -1.71×10^{-13} cm^2/dyne; and the strain-optic coefficient, $p_{11} - p_{12} = -0.100$.

ARPA Order Number:

02413

Program Code Number:

3D10

Name of Contractor:

The Pennsylvania State University

Effective Date of Contract:

25 April 1973

Contract Number:

F19628-73-C-0219

Principal Investigators and Telephone Numbers:

Prof. Bruce E. Knox, 814/865-1168

Prof. K. Vedam, 814/865-1146

AFCRL Project Scientist and Telephone Number:

Mr. Joseph J. Comer, 617/861-4823

Contract Expiration Date:

31 December 1974

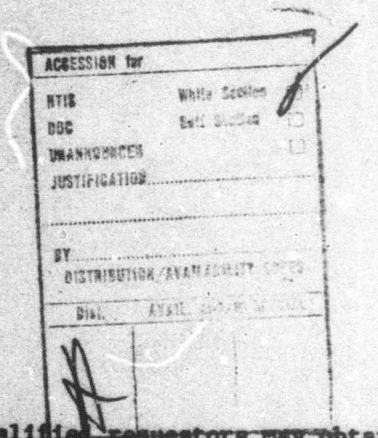

COATING SCIENCE AND TECHNOLOGY

B. E. Knox and K. Vedam
Materials Research Laboratory
The Pennsylvania State University
University Park, Penna. 16802

TECHNICAL SUMMARY

Technical Problem and Methodology

The objective of this research program was to develop a thorough understanding of the science and technology of films applied as coatings on materials transparent to 10.6 and 3-5 micron radiation. The approach included preparation of films by sputtering, evaporation and CVD techniques. The materials considered were inorganics, both elemental and/or compound, with early work on elemental films. Tetrahedral carbon films and organic films formed by plasma polyermization were also investigated. Techniques for characterizing the films included, IR spectroscopy, laser Raman spectroscopy, SEM, electron microscopy, x-ray emission analysis, ion scattering spectrometry, Auger electron spectroscopy and strain measurements.

Technical Results

An extensive study of the sputter-deposition of germanium films on KCl substrates was conducted. Utilizing the technique of welding the KCl substrates to the heat sink in the sputtering system has allowed us to extend the range of sputtering conditions under which germanium films can be made.

We have studied the oxidation of sputter-deposited amorphous germanium films because of the possible absorption problem at 10.6 μm. Infrared spectroscopy was used to determine that the kinetics of the film oxidation followed a logarithmic rate. Ion scattering spectroscopy was used to study the composition profiles through germanium films and to show that the oxygen is uniformly distributed throughout the entire film, even penetrating into the bulk substrate for some distance as does the germanium. The composition profiles showed a distinct interface covering a region about 100 Å thick. Thus, bulk oxidation of the germanium film occurs, even after a short exposure to air.

Preliminary studies of the sputter-deposition of CdTe on KCl were undertaken. Just as in the case of Ge films the nature of the sputtered CdTe film is found to be strongly dependent on the sputtering conditions. In fact, we can produce

either crystalline (cubic and/or hexagonal) or amorphous films of CdTe simply by controlling the Ar pressure, r.f. voltage and power and the physical geometry of the sputtering target, substrate, etc. Sputtering parameters were found to affect the adherence of the film to the substrate, as revealed by scratch and abrasion tests developed in this laboratory. Auger electron spectroscopy and ion scattering spectrometry studies on such sputtered CdTe films revealed that the surfaces of the films were rich in tellurium and that small amounts of oxygen were incorporated in the surface layers of the film.

A method of determining the "durability" of a film on a particular substrate has been established. This involves: (a) "scratch-test" adhesion measurements, with the critical loads normalized to the substrate hardness; (b) abrasion test measurements; (c) an evaluation of the stress conditions of the film; and (d) analysis of the interface region between the film and the substrate by compositional profiling with ion scattering and Auger electron spectroscopy.

A number of cutting and polishing techniques were investigated for KCl substrates. The specimens were then examined with ellipsometry, a tool which has been used extensively in the studies of both substrate surfaces and films. The degree of damage and the thickness of the damaged layers on substrate surfaces which have been prepared for sputtering have been measured by this technique, thus making it possible to correlate different preparation techniques with certain aspects of film deposition and adhesion. Electron microprobe analyses and scanning electron microscopy have also been utilized widely in the initial preparatory studies.

Germanium films deposited on KCl substrates prepared by various techniques have been subjected to durability testing. Initial results indicate that bonding between the film and the substrate is due to van der Waals forces and not to the chemical nature of the surface.

A study of the factors involving stress in films has been made. Two types of stress may occur, thermal and intrinsic. A stress may either be compressive or tensile, which will cause a film either to buckle up on the substrate or peel back from the substrate. By tailoring the sputtering conditions we can prepare films of germanium on KCl which are either compressive or tensile. This makes it possible to compensate for an expected thermal tensile stress with an intrinsic compressive stress.

Attempts to prepare germanium films on KCl substrates using chemical vapor deposition techniques were not very successful. Under the prevailing reaction conditions, the iodine utilized to transport the germanium to the deposition site (in the form of GeI_2 and GeI_4) also tended to react with the substrate surface, replacing the chlorine and effectively etching the surface. Computer studies of the system thermodynamics showed that no parameters could be changed to enhance the deposition of germanium before the substrate was etched.

Studies to prepare tetrahedral carbon (the so-called "diamond film") were also initiated. It was proposed to laser-evaporate graphite and allow the vapor plume (mainly C_3 and C_1) to pass through a microwave cavity to form atomic carbon before it was deposited on the substrate. Preliminary studies to deposit carbon films by laser evaporation alone were successful, though the films so obtained appeared to be amorphous. However, power densities high enough to produce free jet vaporization could not be obtained with the laser system available in this laboratory. As a result, the use of a CO_2 laser to produce carbon vapor was discontinued.

In response to a request from DARPA we have prepared some organic films by the plasma-polymerization technique using microwave, rather than r.f. excitation. The purpose of such films would be to provide a homogeneous, pinhole-free encapsulation for optical components to protect them from the surrounding environment. A series of films were prepared to find the optimum deposition parameters and examined optically, by scanning electron microscopy and electron microscopy to check their homogeneity. In addition we demonstrated the relative ease with which such films can be prepared.

At the request of the contract monitoring agency, we have carried out experiments to determine the stress-optic coefficient of zinc selenide at 10.6 μm. At this wavelength the stress-optic coefficient, $C_\lambda = -11.9$ Brewsters; the piezo-optic coefficient, $q_{11} - q_{12} = -1.71 \times 10^{-13}$ cm^2/dyne; and the strain-optic coefficient, $p_{11} - p_{12} = -0.100$.

DoD Implications

The results of these studies will be used to provide guidelines for the selection of the best materials, process and process controls for the production of good optical coatings for infrared components at wavelengths of 10.6 and 3-5 micrometers.

Further Research

No further research will be undertaken under this contract. However, this research is being continued under Renewal Contract F19628-75-R-0126.

Specific Comments

No specific comments are offered at the time of this report.

Table of Contents

List of Figures

List of Tables

COATING SCIENCE AND TECHNOLOGY

B. E. KNOX AND K. VEDAM
Materials Research Laboratory
The Pennsylvania State University
University Park, Pennsylvania 16802

1. INTRODUCTION

The objective of this research program was to develop a thorough understanding of the science and technology of films applied as coatings on materials transparent to 10.6 and 3-5 micrometer radiation. The approach included the preparation of films by sputtering, PVD, CVD and plasma-polymerization techniques. Except for the plasma-polymerization studies, only inorganic materials were considered; the initial work was with elemental films of germanium, while more advanced work included the compound cadmium telluride. Tetrahedral carbon films were investigated, as well. The techniques utilized for characterizing the films and substrates included IR and Raman spectroscopy, x-ray emission spectroscopy, scanning electron microscopy, ellipsometry, ion scattering and Auger electron spectroscopy, and strain measurements. The results of these investigations will be used to provide guidelines for the selection of the best materials, processes and process controls for the production of good optical coatings for IR components at the specified wavelengths.

The requirements for good coatings must be thoroughly understood in order to plan a course of study to overcome the problems of absorption and damage to surfaces and coatings on windows used to transmit high intensity infrared laser beams. Antireflection coatings are essential, and coatings to prevent degradation by the atmosphere are often required, as well. In general coated windows must have reflectances less than 0.1%, optical absorption losses less than 10^{-4} per surface, and should be uniform to $\lambda/40$. The coatings must be moisture resistant, cleanable, adherent, and must make good thermal contact with the substrate. Furthermore, the damage threshold of the coatings and surfaces must be as close as possible to the damage threshold of the bulk window materials. With these requirements in mind, one can then proceed to select coatings; with the exception of tetrahedral carbon, the two-layer systems of

Loomis (1) have been assumed to be the best solutions for those problems. Figure 1 details the first phase effort in our Laboratory.

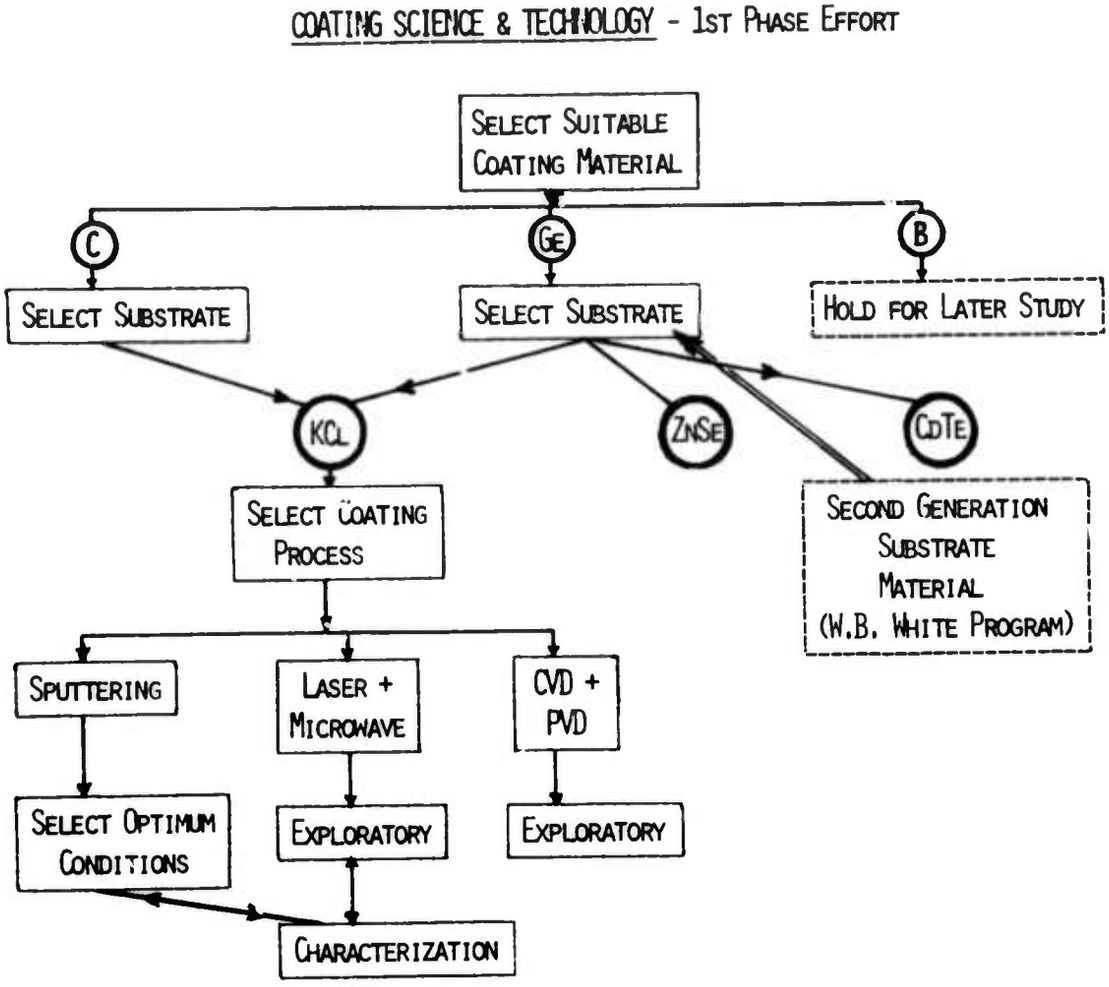

Figure 1. Flow diagram of coating-research effort at Penn State University.

2. SELECTION OF MATERIALS

2.1 Antireflection Coating - First Layer Film

According to Loomis (1) there are a wide variety of combinations of optical films which will act as antireflection coatings on infrared transmitting substrates. One first layer film that can be used to advantage with the most reasonable choices of substrate (e.g., KCl, KCl/KBr, CdTe, ZnSe) is germanium. An extensive amount of work has been done on the preparation and characterization of non-crystalline sputtered germanium films in our Laboratory; this knowledge can be utilized in the present study and thus can result in a

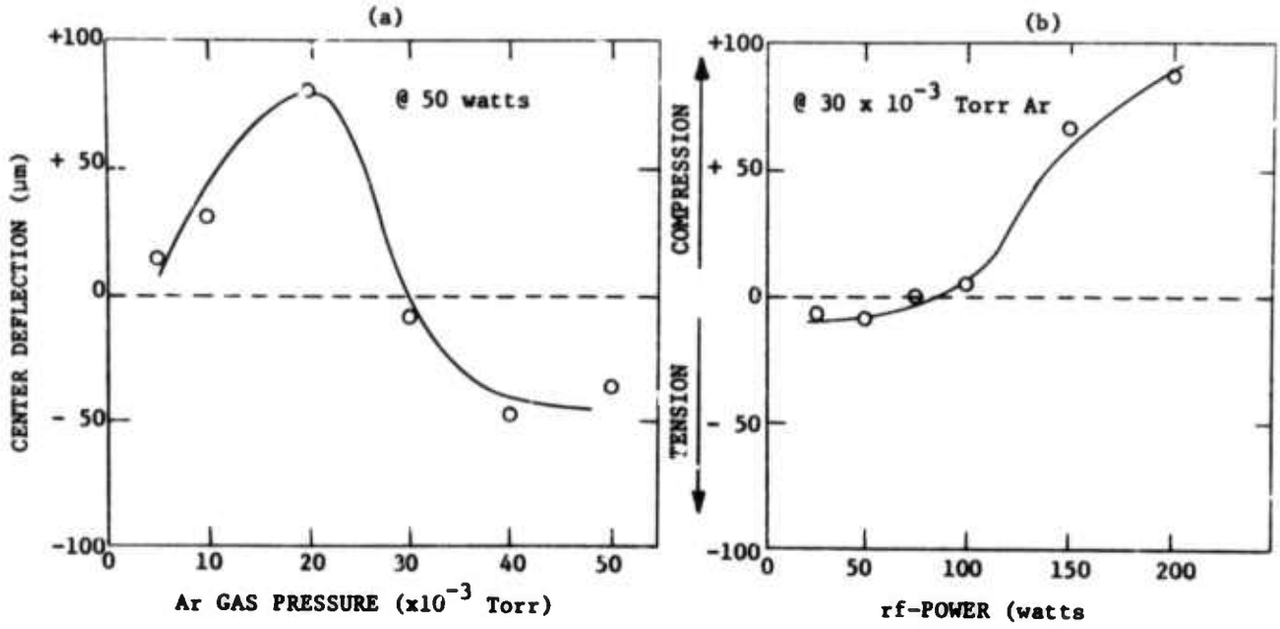

Figure 2. Plot of macroscopic film stress as a function of (a) argon gas pressure, and (b) rf power.

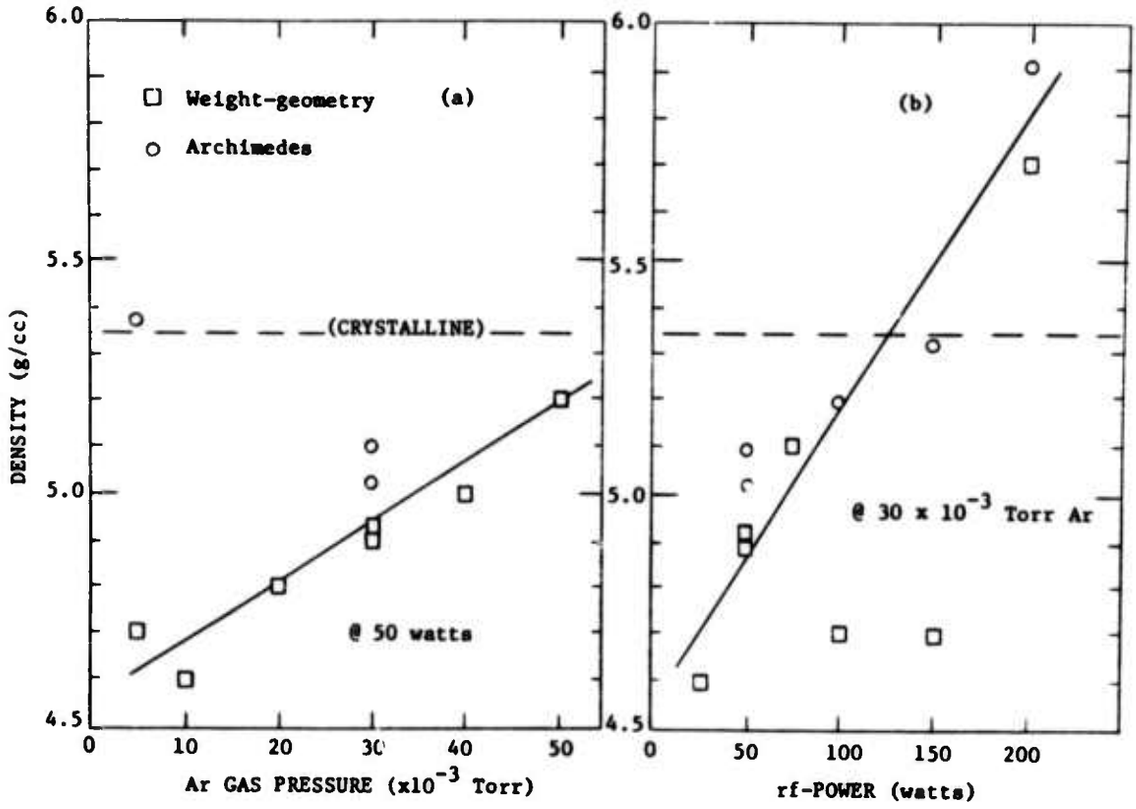

Figure 3. Plot of film density as a function of (a) argon gas pressure, and (b) rf power.

considerable saving of time. For instance, the macroscopic stress in a germanium film can be varied from tensile to compressive (Figure 2); the film density can be varied over a range of 25% (Figure 3); and even the argon content (inherent in the sputtering technique) can be varied from less than 0.2 to more than 5 atom percent, all as a result of varying just two of the sputtering parameters, rf power level and sputtering gas pressure (2). Thus, germanium was selected as a first-layer film to be deposited during the initial stages of this project.

Cadmium telluride is another material that can be used as the first-layer of a two-layer antireflective coating on KCl substrates. However, it does not oxidize as readily as germanium, nor is it limited by thermal runaway problems. Just as with germanium, the nature of a sputter-deposited CdTe film is strongly dependent on the sputtering conditions used in its preparation.

2.2 Substrate Materials

With germanium as a first layer film, several substrate materials can be used such that the specific coating characteristics mentioned earlier in this paper are satisfied. The choice was narrowed to three: KCl, ZnSe, and CdTe, based on information provided by Loomis (1), papers presented at the Conference on High Power IR Laser Window Materials held in 1972, and prior experience with the materials, themselves. KCl was chosen as the substrate for first phase studies for a number of reasons. These included availability, cost, ease of handling and ease of polishing.

2.3 Second Layer Film Materials

Having chosen the first layer film and the substrate, the choice of second layer film is more restricted. Even though many materials will satisfy the optical criteria for a second layer film, one additional requirement narrows the choice considerably. Because of the nature of the sputtering process and the inability to control film thicknesses precisely, and also because film thicknesses will change due to natural environmental degradation, the effect of film thickness variation on the reflectivity of the system must be considered an important criterion in the selection of film materials. Table I, compiled from information given by Loomis (1), shows possible second layer film materials over a first layer of germanium on three different substrates and for a first layer of cadmium telluride on KCl. These film materials were chosen on the basis of the insensitivity of their reflectances

TABLE I

ANTIREFLECTION COATING FILMS ON DIFFERENT SUBSTRATES

First Layer Thickness Tolerance ± 3 to 5%

Absorption <0.1%

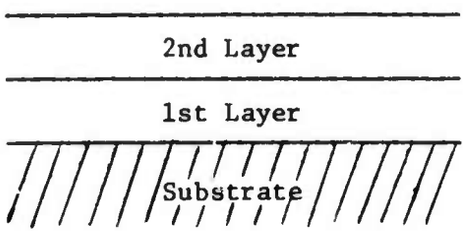

Substrate	1st Layer	2nd Layer
KCl	Ge	ZnTe
		GaAs
	CdTe	ZnS
		CdS
ZnSe	Ge	ZnS
		CdSe
		As_2S_3
		In_2S_3
CdTe	Ge	ZnS
		ZnSe
		CdSe
		As_2S_3

(From the table compiled by J. S. Loomis)

with relatively large variations in film thickness (±5%). In addition, our Laboratory has had reasonable amounts of experience with most of these potential second layer materials.

3. PREPARATION OF SUBSTRATE SURFACES

3.1 Polishing KCl Substrates

Initially, the KCl substrates were prepared by cutting to size with a string saw using silicon carbide as the abrasive and glycerine as a vehicle. Because the resultant samples were so "dirty", a water polishing step was necessary. Then they were mechanically polished using 1 micron alumina with methanol, washed with ether and then chemically polished. The chemical polish-

ing was accomplished by immersing the KCl for one minute into a stirred solution of concentrated HCl; the crystals were held by platinum-tipped forceps to prevent contamination by iron. Then they were immediately rinsed with ether and stored under ether until use. Prior to use, the ether was evaporated from the substrate with a flowing stream of dry nitrogen; the crystals were then heated with an infrared lamp to a temperature between 50° and 60°C for one hour.

To avoid contamination of the cry tals during the cutting stage, they are now being cut with a nylon string saw using water as the wetting agent. With these substrates the initial water polishing step is omitted. After chemical polishing, the substrates are either used directly or subjected to reactive atmosphere processing in CCl_4. The technique has been described by Pastor and Braunstein (3). It consists of placing the substrates in an evacuated chamber, admitting 100-120 torr of CCl_4 at room temperature, and heating to about 670°C for about 20 hours.

3.2 Characterization of Substrate Surfaces - Ellipsometry

As a result of the 1973 ASTM Conference on Laser Damage in Infrared Window Materials, it is now evident that surface irregularities such as submicroscopic cracks, pits, and grooves on a scale larger than about 0.01 micrometer play the dominant role in lowering the surface damage threshold. Thus, surface characterization is essential after every operation in the preparation stage.

For such non-destructive characterization, the ellipsometric technique has been found to be quite useful and informative. As is well known, the ellipsometric parameter, Δ, is most sensitive to the thickness or the growth of non-absorbing contaminant films (4,5), while the parameter, ψ, is dependent on the degree of perfection of the substrate itself, i.e., on the dislocating density in the surface layers of the substrate (6) as well as on the surface roughness (7).

Table II lists the observed values of Δ and ψ for various samples of potassium chloride with different preparative histories. The values of Δ and ψ, calculated with the help of exact equations of ellipsometry for the ideal case of KCl substrate free of damaged surface layers as well as contaminant film, is also entered in the table.

Table II

Ellipsometric Parameters for Potassium Chloride Substrates as a Function of Surface History

λ = 5461Å n = 1.4939 ϕ = 58°

Surface History	ψ (deg.)	Δ (deg.)	Damaged Layer n_2'	Damaged Layer d_2' (Å)
Ideal Case	2.82	0.00	-	-
Cleaved	2.89	1.07	1.492	660
Cleaved + Annealed	2.83	2.47	1.493	50
Mechanically Polished	4.99	19.51	1.440	680
Mechanically + Chemically Polished	2.90	2.45	1.489	420
Mechanically + Chemically Polished; Annealed	2.91	2.84	1.488	330

It is seen that the value of ψ (which can be determined to ± 0.02°) measured on the cleaved sample of KCl is quite different from 2.82°, the value corresponding to the ideal case. If this difference is associated solely with the presence of a damaged surface layer on the substrate, then the effective thickness and the refractive index of such a damaged layer can be evaluated, and such values also are entered in the table. It must be emphasized that no great significance should be attached to these values, since the effect of surface roughness has been ignored in such calculations. On annealing these cleaved samples at 670°C for 20 hours in CCl_4 atmosphere (following the reactive atmosphere processing procedure described by Pastor and Braunstein (3)), it is seen the ψ_{obs} approaches that of the ideal case, indicating that the surface is free of a damaged layer and/or surface roughness. However, it is not always possible to reproduce such a sample by cleaving procedures, since the number and distribution of cleavage steps and tear lines with accompanying dislocations near the surface cannot be controlled.

Hence, in order to obtain specimens in a reproducible fashion, they were cut from blanks obtained from Harshaw Chemical Company into the desired shape with the help of a nylon string saw using water as the wetting agent. Then the specimens were mechanically polished flat with Linde A (Al_2O_3) compound. Since the surface layers of such a mechanically polished sample will be highly strained, it is necessary to chemically polish them in concentrated HCl at

room temperature for about 1 minute to remove the damaged layers. This is evident from the enormous decrease in the observed value of ψ on the chemically lished sample from that of the mechanically polished specimen (Table II). However, the value of ψ obtained on such chemically polished specimens is still far from the ideal value. Annealing at high temperatures in CCl_4 atmosphere also did not improve the situation. Experiments with a number of other specimens with similar treatments but with varying degrees yielded almost similar results.

It may be recalled that in the case of silicon (n = 4.050, k = 0.028), almost identical values of $\psi(=\psi_{ideal})$ were obtained by chemical polishing treatments, even though they were carried out by different workers. Thus, it appears that in the case of silicon the surface roughness does not play a dominant role in affecting the value of ψ, provided, of course, the roughness is not too coarse (7). The present experiments on KCl indicate that we cannot generalize from the results of silicon, that for all materials with $k << n$, ψ depends mainly on the damaged surface layers and not on the surface roughness. Since the KCl crystals used in the present studies were not "special window grade" specimens, it is likely that the chemical polishing may have been uneven across the face of the specimen, particularly near the small angle grain boundaries, thus creating a microrough surface. Currently, experiments are in progress with "window grade" specimens to verify the above hypothesis. Further, the samples are also being irradiated with γ-rays to radiation-harden them (8) and thus reduce the damage introduced during the mechanical polishing stage. The point defects introduced by radiation will be annealed out during the subsequent annealing stage. Once the effect of surface roughness is understood and overcome, the damaged introduced in the surface layers during deposition of the antireflecting layer can also be monitored and thus controlled.

3.3 Sputtering Conditions for Alkali Halides

The first problem to be solved was the sputtering away of the alkali halide substrate, itself, by the high energy electrons striking its surface. This problem is peculiar to alkali halides and is caused by high energy electron generated defects called V_k centers. The defect dissociates, ejecting a halide atom, leaving the metal atom to evaporate. The result is an extremely rough surface which is incompatible with optical-grade materials.

Neither the use of an rf inductor between the substrate and ground nor the use of a magnet to divert the electrons from striking the substrate proved to be effective in reducing substrate sputtering.

Three solutions to the problem were found: (a) using a combination of high system pressure (>30 mtorr), large target-to-target substrate (>10 cm), and low sputtering power level (<50 watts); welding the substrate to its holder with gallium metal; and welding the substrate to its holder with water. The welding techniques serve to provide better heat transfer between the substrate and holder, thus removing energy from the substrate and decreasing the damage caused by the sputtering plasma. Water dissolves a small amount of the surface, which subsequently recrystallizes, bonding the substrate to the heat sink. Using this technique we were able to prepare germanium and cadmium telluride films under a wide range of conditions without the risk of contaminating the films with gallium.

4. FIRST-LAYER FILMS OF GERMANIUM ON POTASSIUM CHLORIDE SUBSTRATES

4.1 Sputter-deposition of Ge on KCl

Since the conditions for making germanium films with a wide range of properties had already been done in this laboratory, the only problem to be solved was that of the substrate being sputtered by the plasma. Using the water-welding technique described above, many films were made for subsequent characterization and durability testing. The results of these operations will be described in later sections.

4.2 CVD Deposition of Germanium

Vapor transport methods for depositing coatings can make use of thermodynamic data in calculating the limiting rates of deposition and in determining which chemical reactions are important as a function of temperature and pressure. We utilize a special computer program for the calculation of complex chemical equilibria as functions of pressure and temperature. These calculations provide the basis for the selection of feasible chemical vapor deposition reactions and the optimum experimental conditions under which to conduct them.

Germanium is suitable for the first coating, as has been mentioned above, and it can be deposited at "low" temperatures of about 300°C. We have constructed a flow apparatus for the preliminary studies of deposition via the germanium tetraiodide reaction scheme. Argon containing vaporized iodine is reacted with germanium metal at about 500°C to produce $GeI_2(g)$ as the principal

product. The diiodide vapor flows past the substrate material which is heated to 200°-300°C, and germanium is deposited as a film. The reactions are as follows:

$$I_2(s) = I_2(g) \qquad 298°K$$

$$Ge(s) + I_2(g) = GeI_2(g) \qquad 800°K$$

$$2GeI_2(g) = GeI_4(g) + Ge(s) \qquad 500°K$$

Computer calculations of the equilibrium in a flow system containing germanium, iodine, and argon were carried out to help explain our experimental results and to provide direction in choosing our experimental parameters. The maximum amount of germanium is put into the gas phase in the form of GeI_2 and GeI_4 at about 500°C in the presence of argon at a pressure of 1 atmosphere, previously saturated with iodine at room temperature. The most important reaction at 500°C is:

$$Ge(s) + 2\ I(g) = GeI_2(g)$$

At higher temperatures this reaction reverses and deposits germanium. At lower temperatures $GeI_2(g)$ decomposes to deposit germanium by the reaction:

$$2\ GeI_2(g) = Ge(s) + GeI_4(g)$$

Thermodynamically, the amount of germanium deposited at low temperatures reaches its maximum value at about 200°C; kinetically, the reaction depositing germanium may have neglibible rates at higher temperatures. Under typical experimental conditions, e.g., an argon flow rate of 56 cc/min., $I_2(s)$ at room temperature and the source Ge(s) at 500°C, we can expect a maximum deposition rate of about 2 mg/hr of Ge at lower temperatures. We chose to use flow rates up to about 200 cc/min and to saturate the argon with iodine held at 60°C in an attempt to quickly deposit a protective film on the KCl. Maximum possible deposition rates calculated for these conditions are on the order of 70 mg/hr.

Two batches of film have been produced by this method. One film was 5.4 μm thick and had the appearance of a very rough surface. It flaked off

the substrate rather easily. This film was identified as a crystalline germanium by x-ray diffraction. The other film was quite thin, but it adhered much better than the first film.

Surfaces of the KCl substrates became "frosted" during the CVD process. They did not become "frosted" when subjected only to a stream of argon containing $I_2(g)$. Electron microprobe analysis showed that the entire surface contained iodine, probably as the iodide replacement for the structural chloride. Only very weak chlorine signals were obtained. A probable reaction scheme for the iodine inclusion is:

$$GeI_4(g) + xKCl(s) = GeI_{4-x}Cl_x(g) + xKI(s)$$

If this is the case, one could expect the formation of all forms of GeI_{4-x}. No conditions were found which would make this type of reaction unfavorable. Thermodynamically, however, we might expect iodine to be even more reactive with ZnS and CdTe.

A small amount of white deposit appeared on and near the source of Ge(s) at the higher temperatures. This deposit was most likely GeO_2, and probably arose from impurities in the argon (although it was dried) and the adsorbed water on the walls of our CVD system. Some germanium may also have been transported to cooler temperatures in the form of GeO(g). A thermodynamic analysis of the effects of water impurity in the system as a function of temperature and various initial H_2O partial pressures was conducted.

Since we had problems with iodine etching the KCl substrates, we also considered other approaches. In particular, the possibility of reducing $GeCl_4(g)$ with $H_2(g)$ to deposit germanium was studied, but the required temperatures for deposition were too high for use with KCl.

4.3 Oxidation of Amorphous Germanium Films

4.3.1 Background

Crystalline germanium has a thin oxide layer on any surfaces exposed to air. The first oxide monolayer forms in approximately 6 seconds according to Green (9); subsequent oxidation proceeds more slowly, following a logarithmic rate law which is common for many metals.

Amorphous germanium films may contain voids which would have the effect of increasing the area of the germanium surface which is exposed to the

atmosphere. Void-free amorphous germanium films have been prepared by e^--gun deposition (10). However, Helms et al. (11) have observed evidence of bulk oxidation from the reflectance spectra of void-free amorphous germanium films. They suggested that bulk oxidation could be due to the openness of the amorphous germanium lattice with respect to the crystalline lattice.

Thus, we conducted an investigation of the oxidation of sputter-deposited amorphous germanium films, because bulk oxidation could seriously impair their usefulness as coatings for laser windows.

4.3.2 Experimental Procedure

The sputtering was carried out using the following conditions: 5 inch germanium target; r.f. voltage - 400 volts; r.f. power - 45 watts; argon pressure - 30 mTorr. Films 1000 Å and 1 μm in thickness were prepared for the oxidation studies.

A Perkin-Elmer model 621 grating infrared spectrophotometer was used to determine the extent of oxidation of the germanium films. Figure 4 shows the most prominent IR peak produced by amorphous germanium dioxide.

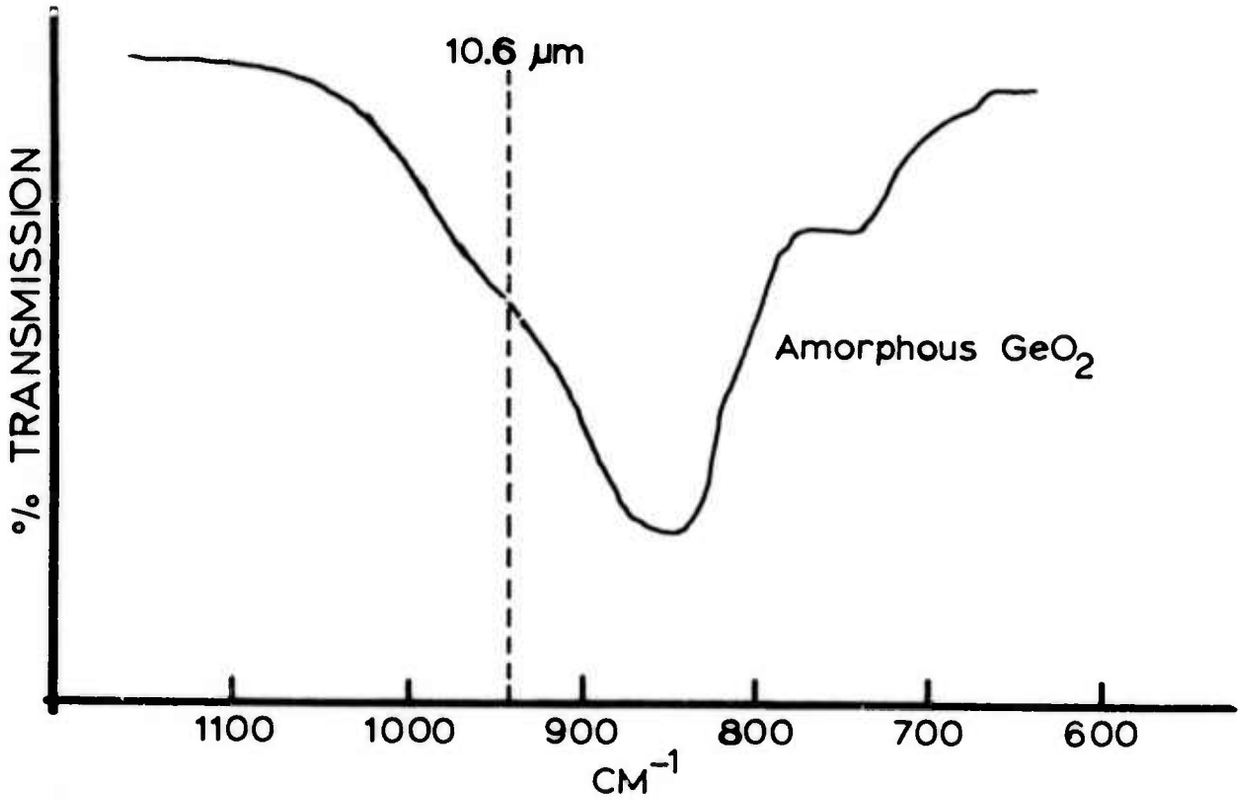

Figure 4. Infrared Spectrum of Amorphous Germanium Dioxide.

4.3.3 Discussion

The principle aim of these studies was to determine the extent of bulk oxidation of amorphous germanium films. Figure 5 shows the percent oxidation versus time for films 1000 Å and 1 μm in thickness exposed to air at room temperatures. The amount of oxidation was determined from the IR peak height at room temperature and the peak height for a completely oxidized film. Complete oxidation was easily attained by heating in air at temperatures $\geq$ 510°C. Table III shows results from electron microprobe studies which indicate the formation of GeO_2 from amorphous germanium films at heating times of less than one minute.

Table III

Electron Microprobe Analyses of Oxidized Amorphous Germanium Films*

Sample	Element	Composition (atom percent)
1	Germanium	31.2
	Oxygen	68.2
2	Germanium	27.4
	Oxygen	72.6

*One micrometer germanium films on KCl: 2 inch target, r.f. voltage - 380 volts; r.f power - 25 watts; argon pressure - 30 mTorr. Films heated in air for approximately 1 minute at 519°C. Sample 1 substrate irradiated with gamma rays from a cobalt 60 source (2.4×10^7R) to increase hardness before mechanical and chemical polishing.

The curves shown in Figure 5 have the typical shape of oxidation curves following a logarithmic rate law. The rate of oxidation becomes very slow at approximately 25% oxidation for the 1000 Å films. This degree of oxidation is not likely for a single oxide layer on the top surface of the film. The 1 μm film attained a slow rate of oxidation at approximately 12% oxidation. If only top surface oxidation of the film were occurring the 1 μm film should have attained only 2.5% oxidation.

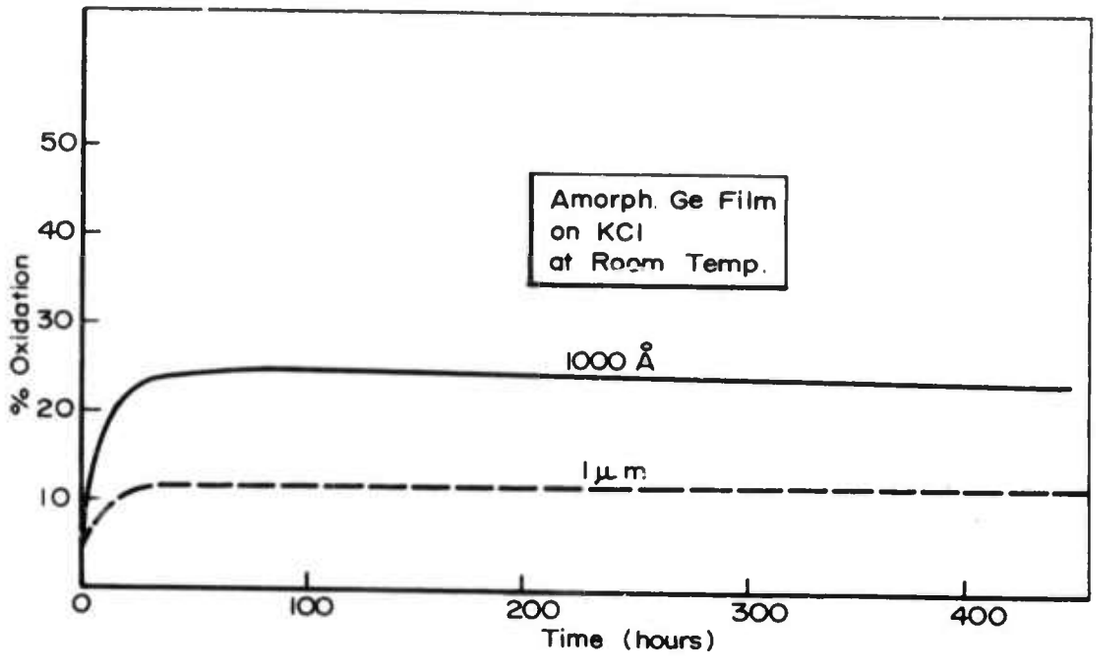

Figure 5. Oxidation of Amorphous Germanium Films at Room Temperature.

Figure 6 shows the oxidation curves for 1000 Å and 1 μm heated at 150°C and 300°C. The oxidation shown in these curves is in addition to the room temperature oxidation. Again, the curve shapes suggest a logarithmic rate law. The logarithmic rate, the large degree of oxidation, and the relative

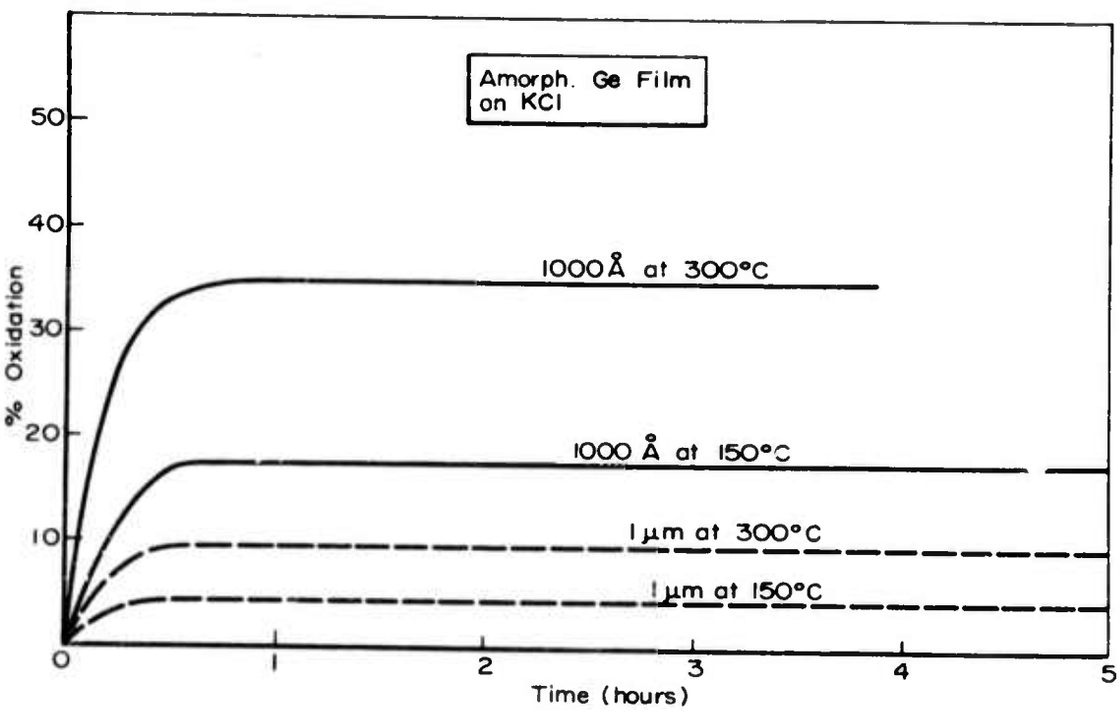

Figure 6. Oxidation of Amorphous Germanium Films at 150°C and 350°C.

amounts of oxidation for the 1000 Å and 1 μm thick films all indicate that a large amount of bulk oxidation of the film must occur, even at room temperature.

One monolayer of amorphous germanium dioxide is 3.66 Å thick (12). Thus, a 1000 Å germanium film 25% oxidized would have approximately 68 monolayers of GeO_2, or 1 monolayer for every 14-15 Å of film, assuming that the oxidation is uniform throughout the film.

4.3.4 Ion Scattering Profiles through Germanium Films

In an attempt to better understand the oxidation of germanium films, compositional profiles were obtained by ion scattering spectroscopy. He^4 was used as the scattering gas, and the sputtering rate was approximately 40 monolayers/hour. The sputtering rates were not quite the same for the two samples profiled; hence, the two sets of data were normalized to a constant sputtering rate and plotted together. Figure 7 shows the normalized composition profiles of germanium, oxygen, and a combined "species" labeled argon, potassium and chlorine. Since the masses of these elements are very close together, it is difficult to differentiate between them using the ion scattering technique.

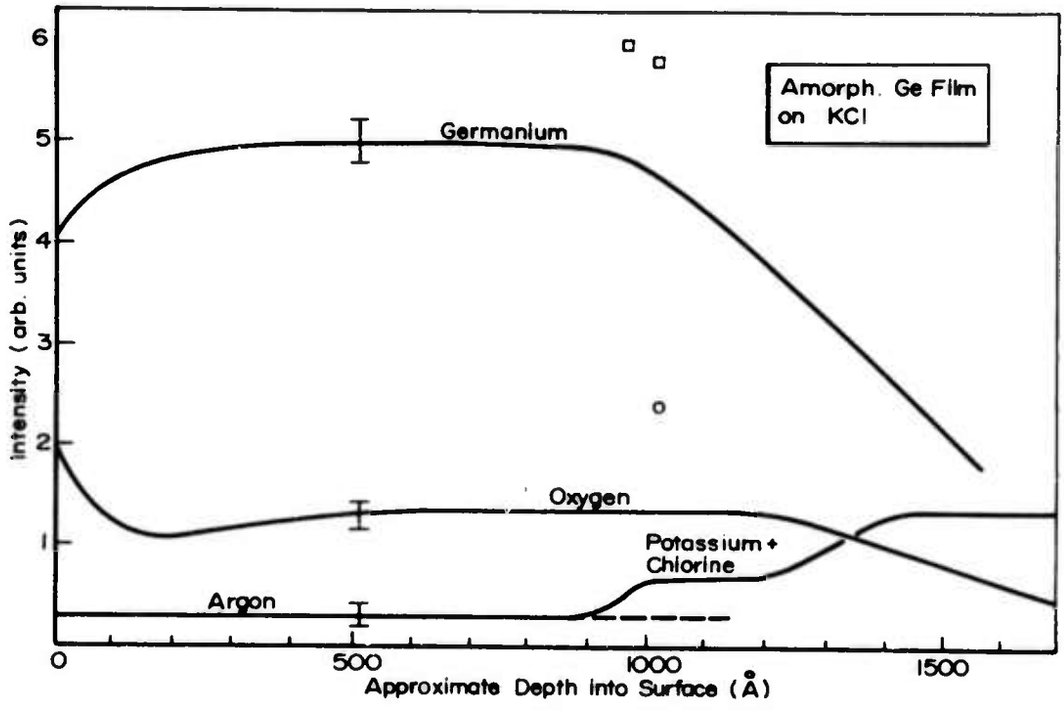

Figure 7. Ion Scattering Profiles through Amorphous Germanium Films.

Near the surface there is a higher concentration of oxygen. This is probably due to a combination of absorbed oxygen and an increased degree of oxidation. There is a corresponding decrease in the germanium concentration. Since these films were prepared by an argon sputtering process, one expects to find argon distributed uniformly through the film, as is the case here. There is clear evidence of some sort of interface at about 1000 Å, the thickness of the deposited film. This is shown by a marked increase in the germanium and oxygen content (shown by separate points above the general lines in Figure 7) and by a shoulder on the argon-potassium-chlorine line. The germanium concentration begins to fall off at this point, but the oxygen remains essentially constant for another 200 - 300 Å. At this point the argon-potassium-chlorine line exhibits another shoulder before attaining a constant value.

The double-shouldered argon-potassium-chlorine line can be explained in the following manner. It is well known that electron and ion beams cause KCl to dissociate. The chlorine diffuses out, leaving a potassium-rich surface layer. The first shoulder corresponds to the location of the original surface of the KCl substrate and, hence, the beginning of the potassium-rich layer. The oxygen appears to fill the vacancies left by the chlorines in the lattice. The second shoulder marks the end of the beam-damaged region and the beginning of the bulk substrate material. Note that some oxygen apparently has diffused into the substrate for hundreds of Angstroms and that germanium apparently has been implanted by the sputtering process and possibly by diffusion for a very great depth, as well. The profiling experiments were terminated after approximately 10 hours, and the germanium and oxygen concentrations were not followed to the point of non-detectability. However, these low concentrations of oxygen and germanium could have been caused by a "crater" effect, i.e., small signals for both oxygen and germanium were detected from the sloping sides of the crater formed by the primary ion beam. Addition of a raster-scan system for the primary beam will give signals derived only from the center of the crater, thus eliminating any possibility of signals being derived from the crater walls.

4.3.5 Conclusions

The results presented from the infrared studies of oxidation rates, the ion scattering profiles, and the electron microprobe analyses of germanium films all show that amorphous germanium films tend to oxidize, not

only on the surface, but also in the bulk. If germanium is to be used as the first film in a two-film antireflective coating, the second film must be deposited before the germanium is exposed to any oxygen. Even if this precaution is taken, oxygen diffusion through the second film could produce the undesirable germanium dioxide, thus degrading the optical quality of the coating.

4.4 Compositional Profiling of Ge Films

Ion scattering has been used to study the compositional profiles of germanium films on KCl. In the previous section, we presented the results of studying films which had been heated in air to enhance their oxidation. In addition we have studied germanium films which have been allowed to oxidize at room temperature.

It is not feasible to use Auger electron spectroscopy to study thin films deposited on alkali halide substrates. Apparently, the electron beam induces diffusion currents by localized charging effects. This results in potassium diffusing completely through the film, as well as the preferential elimination of chlorine in some form. The exact mechanism is not clear. If, for example, the surface of a pure potassium chloride substrate is examined by AES, the signal resulting from the potassium Auger electrons soon dominates the spectrum, and the chlorine Auger electron signal disappears completely. Thus, all profiling studies have been conducted using ion scattering spectrometry.

Germanium films approximately 1000 Å thick were sputtered on KCl substrates from a 5-inch target using 200 volts r.f. and an argon pressure of 30 μm. They were allowed to sit in a laboratory environment exposed to air for approximately one week prior to insertion in the ultrahigh vacuum system of the spectrometers.

The same general phenomena were observed as in the case of the forced oxidation of germanium films. The surface is slightly oxygen rich and germanium deficient. There is a diffuse gradient of germanium, oxygen and potassium-chlorine-argon at the film-substrate interface. Germanium appears to have been driven into the substrate during the sputtering process, either by the energetics of the deposition process, by diffusion or by a combination of the two.

The oxygen content of these films was somewhat lower than that in the forced oxidized films. However, oxygen appears diffused rather uniformly into these films, just as in the case of the oxidized films. No quantitative values can be given at this time.

5. FIRST-LAYER FILMS OF CADMIUM TELLURIDE ON POTASSIUM CHLORIDE

5.1 Preparation of Sputter-Deposited CdTe on KCl

All films were sputtered from a 5" CdTe target in an MRC r.f. sputtering system. The CdTe in the hot-pressed target was found to be cubic. The substrate-target distance was 52 mm. Initial pressures were at least 3×10^{-6} torr before the Ar sputtering gas was admitted to the chamber. The r.f. voltage and Ar pressure were varied (200 - 800 volts and 5-40 μm, respectively), to determine what influence they would have on film properties. Substrates included in each run were (1) a glass microscope slide, (2) two cleaved and chemically polished KCl substrates and (3) two mechanically polished and chemically polished KCl substrates. All KCl substrates were attached to the platten with a thin film of water to provide good thermal contact. All films on KCl were then stored in a dessicator until required for further measurements.

Figure 8(a) represents the variation of film deposition rate with the r.f. power at various pressure levels of argon. In general the deposition rate increases as the r.f. power increases. Figure 8(b) represents the same data but plotted as a function of r.f. voltage. On comparing Figures 8(a) and (b), though the general trend is maintained in both cases, it appears that plotting the data as a function of r.f. voltage yields a more systematic behavior; hence, in what follows the data are generally presented as a function of r.f. voltage only.

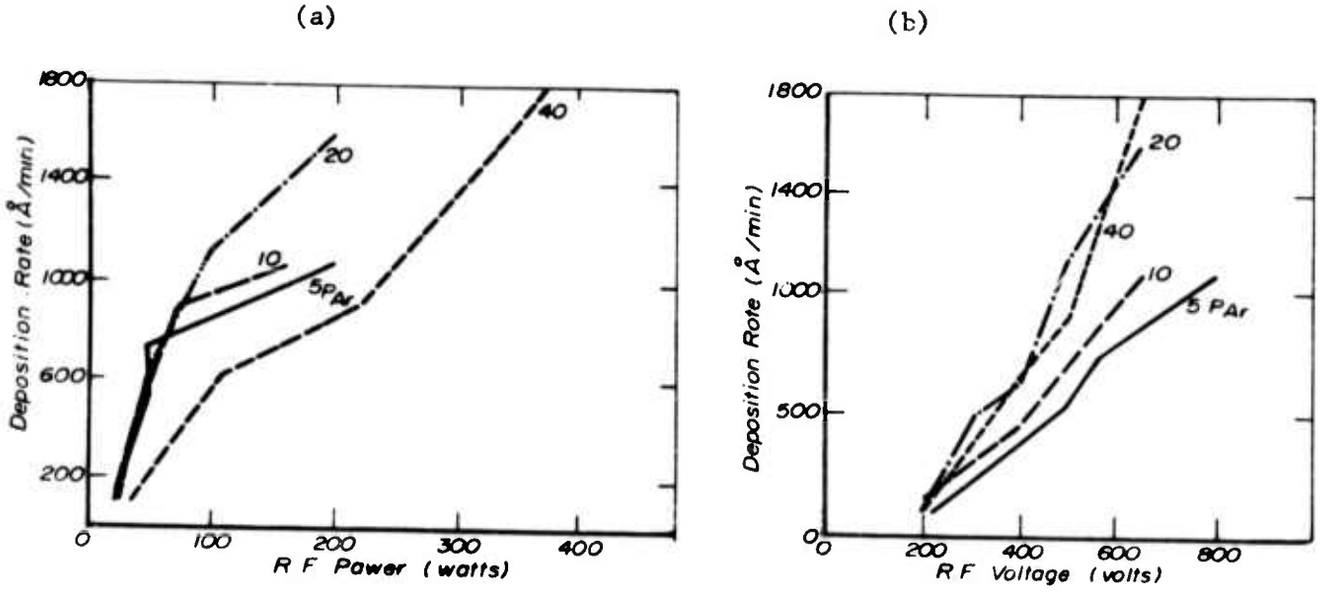

Figure 8. Sputter Deposition Rate of CdTe Films as a Function of (a) r.f. power and (b) r.f. voltage.

5.2 Characterization of Sputter-Deposited CdTe Thin Films

5.2.1 Density Measurement

Thick films varying from 13 μm to 56 μm were deposited on pre-weighed thin glass coverslips. After deposition, the film and coverslips were weighed to determine film weight. Film thickness was determined to ± 0.5 μm by measurement on a fractured edge under a microscope. Area of the film was then measured by a micrometer. The accuracy on density measurements is estimated as ± 0.1 gm/cm^3.

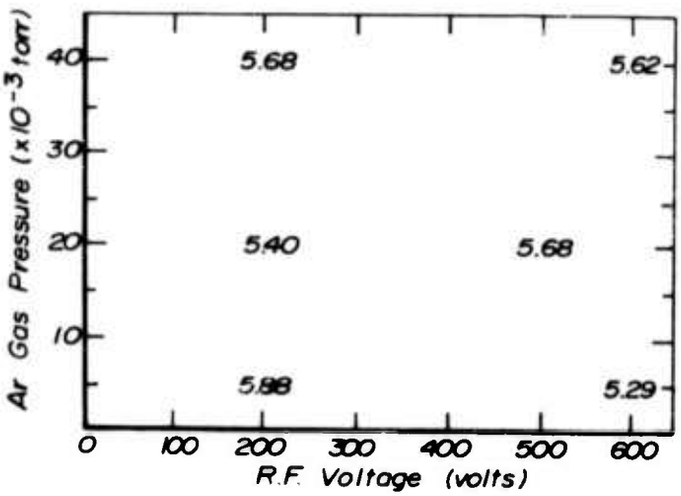

Figure 9. Density (gm/cm^3) of Sputter-Deposited CdTe Films.

The reported density of (hexagonal-cubic) CdTe is 6.20 gm/cm^3 (13) whereas the x-ray density is found to be 5.856 gm/cm^3 (14). All measured film density were between 5.9 gm/cm^3 and 5.3 gm/cm^3, and they are plotted in Figure 9 as a function of the sputtering conditions, r.f. voltage and argon pressure.

5.2.2 X-ray Diffraction

For each run, a film on glass and a film on KCl were analyzed with a GE diffractometer from $2\theta = 10° - 90°$. Those films which showed no diffraction peaks were labeled as amorphous. The value of 2θ, the height, and the full width at half maximum of all peaks were measured. Most films were found to be a mixture of cubic and hexagonal phases; only four films could be identified as completely cubic or completely hexagonal. The hexagonal phase was identified by the (100) reflection at 22.34°, and the cubic phase was identified by the (311) reflection at 46.47°. For all films but one, the major peak occured at 39.4° and could be identified as due either to the cubic (39.34° for (220)) or hexagonal (39.25° for (110)) phase. The intensity of this peak was 10-100 times the intensity of all the other peaks.

This could correspond to preferential orientation with the (110) plane parallel to the substrate if the 39.4° peak were due to the hexagonal phase or (220) orientation if the peak were associated with the cubic phase. The one film which showed only peaks corresponding to the cubic phase had an intensity maximum at $2\theta = 23.8°$, corresponding to the (111) orientation.

Figure 10 represents the crystallinity of the various sputter deposited CdTe films, as a function of r.f. voltage and argon pressure. The symbols H and C indicate that the x-ray diffraction peaks observed for these films could be interpreted as arising from a mixture of hexagonal and cubic phases.

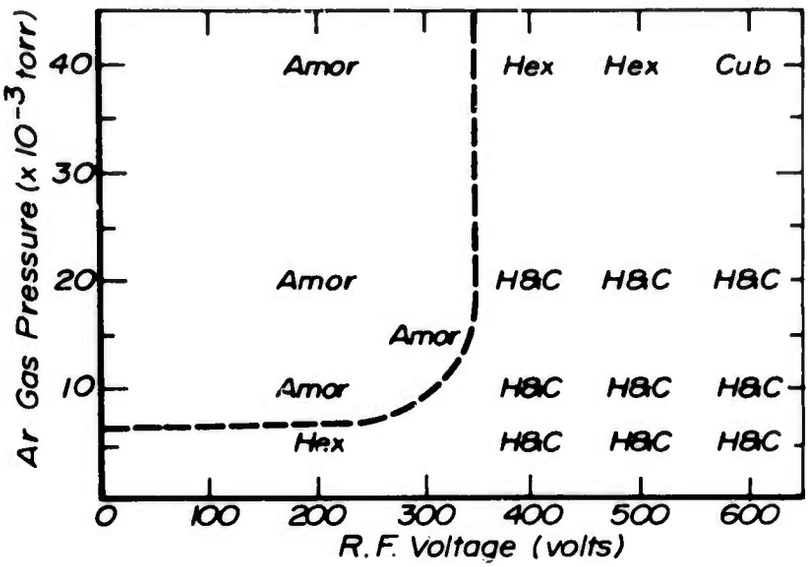

Figure 10. Crystallinity of Sputter-Deposited CdTe Films.

From the half width of the x-ray peaks and their positions, an estimate of crystallite size was made. By assuming that there was no strain broadening, but only particle size broadening, the crystallite size can be determined from the Scherrer (15) equation:

$$D = \frac{K\lambda}{\beta\cos\theta} \text{ , where} \qquad (1)$$

D = crystallite dimension perpendicular to substrate

K = crystallite shape constant assumed to be 0.9

λ = x-ray wavelength

β = corrected line width

θ = Bragg angle

The line breadth was corrected for Kα separation and instrumental broadening after a graphical method of Rau (16).

Figure 11 represents the particle size in Å calculated using the above relation and the 2θ = 39.4 major peak observed in all the films. Figures 12(a) and (b) represent respectively the hexagonal and cubic CdTe particles in the

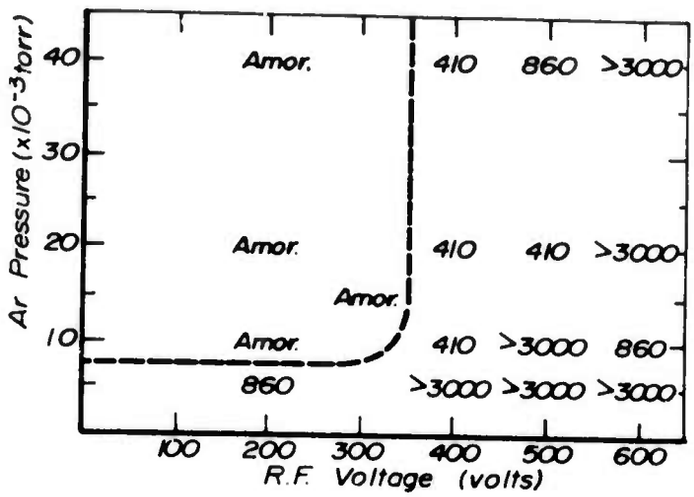

Figure 11. Particle Size (Å) in CdTe Films Sputter-Deposited on Glass Using the 2θ = 39.4° Peak.

(a)

(b)

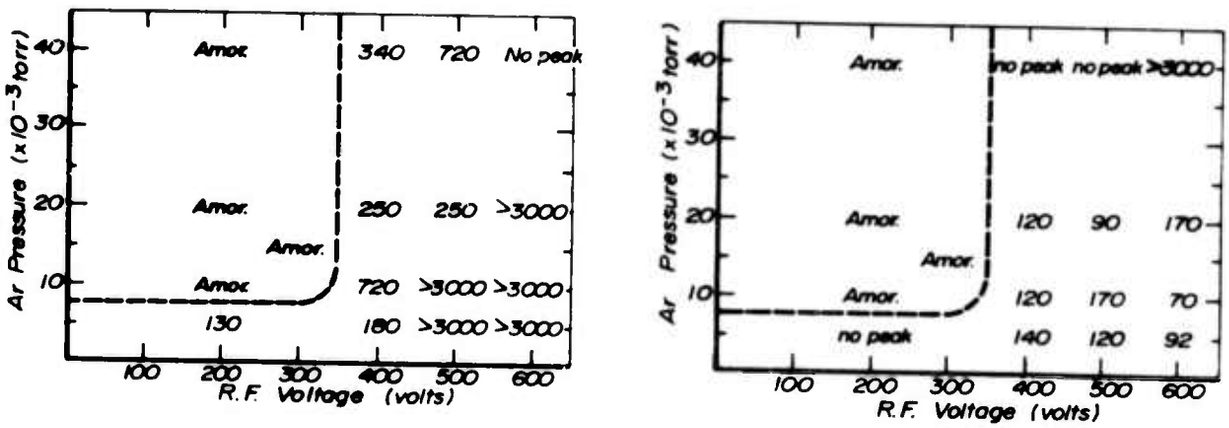

Figure 12. Particle Size (Å) of (a) Hexagonal CdTe and (b) Cubic CdTe in Sputter-Deposited CdTe Films on KCl.

films. From Figure 11 it is seen that in general lower r.f. voltage yields smaller size crystallites. As the r.f. voltage was decreased to 350 volts or less, the particle size became less than 100 Å; such films have been labeled as amorphous. On comparing Figure 11 with Figures 12(a) and (b), it is seen that whenever films of mixed hexagonal and cubic phases are obtained they are mainly composed of the hexagonal phase. The hexagonal crystallite size consistently decreases with decreasing r.f. voltage. On the other hand, the crystallites of the cubic phase do not exhibit any such clear trend. It must be mentioned that the particle size analysis technique used above yielded meaningful results between 100 Å and 3000 Å; for crystallite size larger than 3000 Å the line broadening was not appreciably larger than the instrumental broadening.

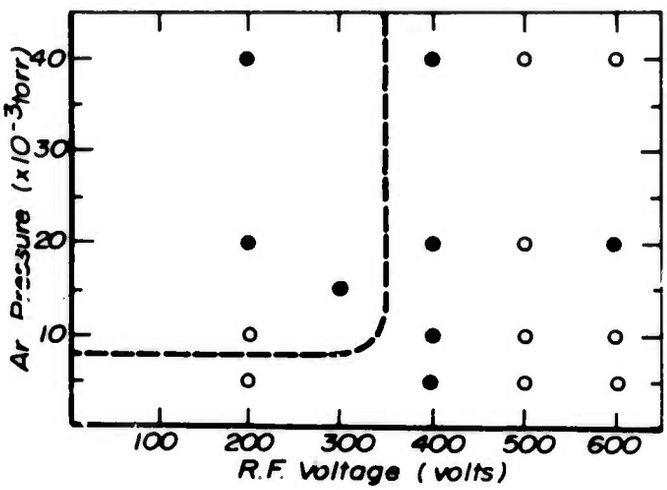

Figure 13. Observation of Spurious Diffraction Peak at 2θ = 38.4° from Sputter-Deposited CdTe Films on KCl.

About half of the films deposited on KCl exhibited one sharp diffraction peak at 2θ = 38.4° which could not be identified as either due to KCl or any phase of CdTe. They are shown in Figure 13 as closed circles, while the open circles indicate that no such spurious peaks were detected on films prepared under those conditions.

The presence of such extra or spurious reflections have been observed (17-19) in electron diffraction patterns from thin films of CdTe or NaCl or mica. These spurious reflections have been attributed to the presence of stacking faults in these films. Efforts are now under way to ascertain whether such stacking faults can account for the observed spurious reflection in the x-ray diffraction pattern as well.

5.2.3 Compositional Analysis of CdTe Thin Films

5.2.3.1 Electron Microprobe Analysis

The CdTe films were analyzed for Cd, Te, and Ar content with an ARL microprobe. The results were corrected for backscatter, absorption, etc. by means of Colby's MAGIC IV computer program (20). The results were studied with respect to the sputtering parameters, and several correlations were obtained, as shown in the following figures.

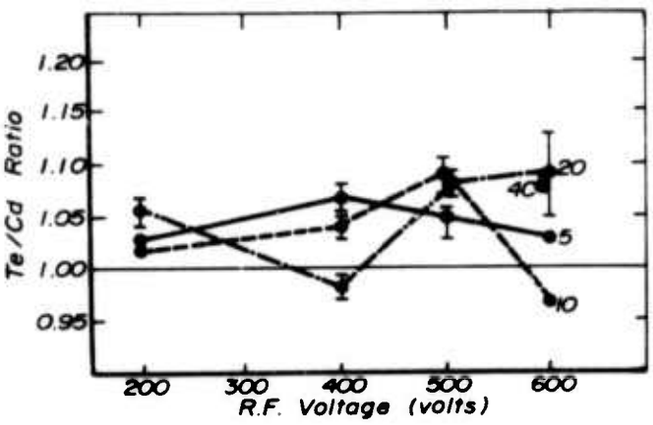

Figure 14. Te/Cd Ratio in Sputter-Deposited CdTe Films on KCl.

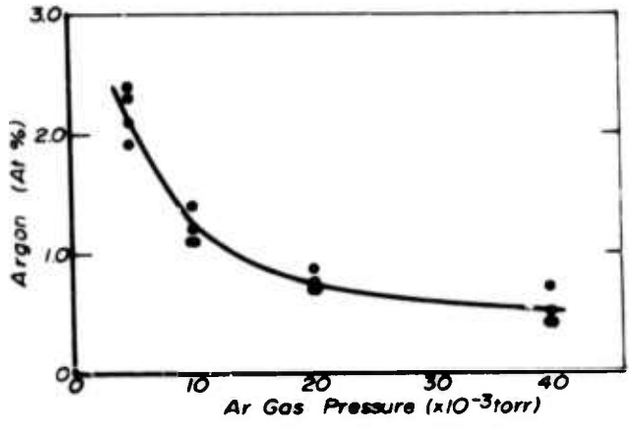

Figure 15. Argon Content of Sputter-Deposited CdTe Films on KCl.

Figure 14 indicates that all samples appear to be Te rich with an average Te/Cd ratio of about 1.07. There seems to be no correlation between the Te/Cd ratios and the r.f. voltage or any other parameter. This may be due to the narrow range of the values and the errors associated with each value. The error bars shown indicate the worst possible case values. They reflect instrument instability, focusing errors, and compositional variations within a given sample. Figure 15 indicates that the Ar content in the film decreases as the Ar pressure increases. Messier (2) found this to also be true for Ge films. Further it appears that oxygen content in the films increase as the argon pressure is increased, although the absolute values of the oxygen content have not been established yet.

5.2.3.2 SEM Analysis

Some representative films were also examined with a JEOL scanning electron microscope. The surfaces were found to be flawless and free of holes at magnifications up to 3000X. X-ray emission wavelength analysis indicated the possibility of the presence of the following impurity atoms in the film: Al, Ti, Ne and Mg. Efforts are under way to quantitatively establish the limiting values of these impurities.

5.2.3.3 Surface Composition of CdTe on Glass Substrates by AES and IEE

Cadmium telluride coatings have been studied by means of ion scattering spectrometry and Auger electron spectrometry. The preparation of these films has already been discussed. Both methods of analysis showed that the surface of these films is tellurium-rich. Both techniques confirmed the presence of a small amount of oxygen in the surface layers of these films, as well.

5.2.3.4 Depth Profiling by Ion Scattering Spectrometry

Initial attempts to obtain compositional analyses of the surfaces of CdTe films by ion scattering spectrometry showed the films to be tellurium-rich. When the instrument was calibrated using a single crystal of CdTe, the surface of the single crystal also appeared to be tellurium-rich. A closer look at these analyses indicated that the primary ion beam was distilling cadmium from the surface, and that after a period of time, only tellurium remained in the signal-generating portion of the surface. Hence, profiles were determined from the tellurium signal alone.

Figure 16 is a typical depth profile of tellurium in a 900 Å CdTe film on KCl. The signal is reasonably constant through the film, with a rather sharp decrease at the interface. The long tail is attributed to a "crater effect", i.e., a small signal resulting from the walls of the crater formed by the ion sputtering process. Modifications will be made to the existing ion scattering/Auger electron spectrometer to eliminate these undesirable effects.

5.2.4 Durability Testing of CdTe Thin Films

A scratch test (Section 8) was performed on CdTe films sputter-deposited on KCl. The values listed in Figure 17 are for the complete removal of the film and are accurate to ±30 gms. For comparison, a load of only 95 gms was sufficient to remove germanium films on KCl. The adhesion of amorphous films was somewhat lower than that for crystalline films.

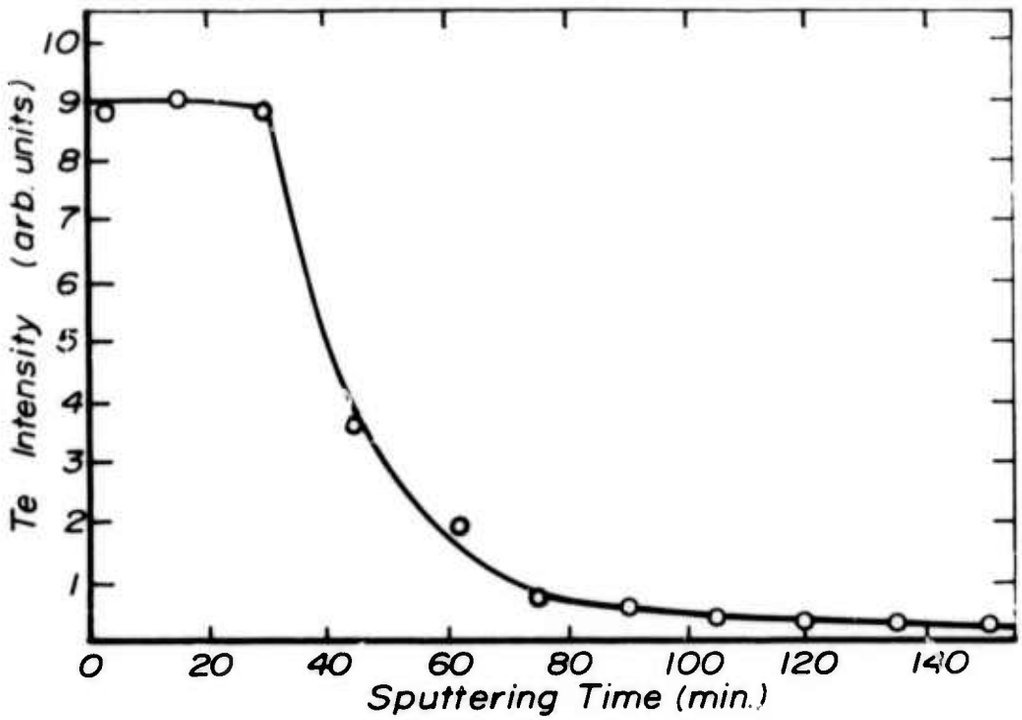

Figure 16. Tellurium Depth Profile of Hexagonal CdTe Sputter-Deposited Film 900 Å on KCl.

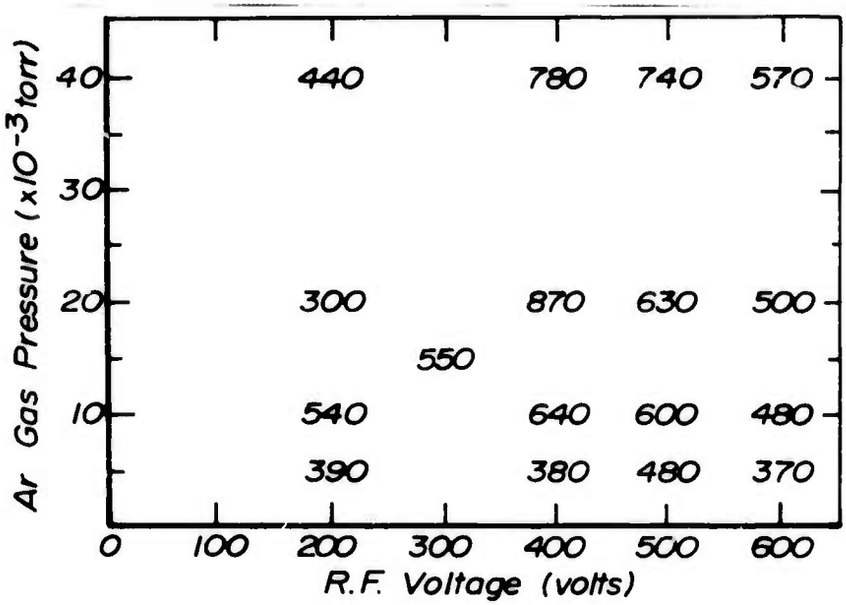

Figure 17. Load (gms) Necessary for Complete Removal of Various CdTe Films from KCl by the Scratch Test.

5.3 Thermodynamics of the Oxidation of CdTe

Oxidation of thin films of CdTe could degrade the optical transparency of laser window coatings at 10.6 μm. The oxidation of CdTe may be written as:

$$CdTe\ (c) + 3/2\ O_2\ (g) \rightarrow CdO\ (c) + TeO_2\ (c).$$

Using data from reference (21) for $G^{\circ}_{F(298)}$ for both reactants and products, we find $G^{\circ}_{298} = -97.2$ kcal/mole. Thus, the above reaction is thermodynamically favorable. The oxidation of CdTe may be limited kinetically, i.e., by a protective oxide layer on the surface. However, thin films may have a very large surface area or a high porosity which would allow bulk oxidation of the film. This has been verified experimentally for germanium films. Sputter-deposited CdTe can be prepared either as amorphous or crystalline CdTe. Thus, it is recommended that the CdTe film which is to be used as a laser window coating be examined for evidence of oxidation.

6. TETRAHEDRAL CARBON FILMS

6.1 Background

One of the most promising film materials for operation in the 10 micrometer range is tetrahedral carbon or the so-called "diamond film." These films have been observed by mass spectrometrists for many years and appear inside their ionization chambers as a result of hydrocarbon fragmentation and pyrolysis within the spectrometer sources. Surprisingly, almost no systematic investigation of these films has ever been done, to the best of our knowledge. Many investigators have confirmed the tetrahedral nature of these carbon films but little else has ever been done. Aisenberg and Chabot (22) used an ion beam technique to deposit films with characteristics similar to carbon in the diamond form, but the structure was never reported. Fedosev et al. (23) reported the fractionation of carbon isotopes in the synthesis of epitaxial films on powdered diamond substrates from methane pyrolysis. Angus, Will and Stanko (24) also reported the growth of epitaxial diamond films on powdered diamond. Since the method of formation of these films is still a mystery, a number of techniques are being explored to grow the tetrahedral carbon films.

Our intent on outset of this project was to laser evaporate graphite and allow the plume of evaporated species (mainly C_3 and C_1) to pass through a microwave cavity in an attempt to predominately form atomic carbon which we hope might form diamond structure carbon on our substrate. We are working with the knowledge that diamond structure carbon has been found as deposits in mass spectrometer sources.

A 50 watt continuous wave CO_2 laser with $\sim$6.3 mm beam diameter was used for vaporizing the graphite. Focusing was accomplished from outside the evacuated evaporation chamber using a 10° focal length antireflection coated CdTe lens. The chamber window material was sodium chloride. The flux density was in the region where the evaporation could be described as 'effusive'. Specifically, with our 10° focal length lens and 6.3 mm diameter beam of 50 watts we could theoretically get a maximum laser flux of 6.4×10^3 watts/cm^2.

Calculations show that this laser flux is too small to overcome thermal conductivity effects and, indeed, experimentally, the vaporization rate was found to be dependent on the mass of the graphite sample. The calculated minimum laser flux density required to produce vaporization with negligible thermal conductivity effects is $\sim 5 \times 10^5$ watts/cm^2. This is the region of free jet evaporation. A lens of shorter focal length could give us this density with our present setup but we would, however, have other problems with the anti-reflection coatings on the lens. For effective evaporization of graphite with the maximum theoretical laser flux available to use, we can use only a sample in the 1-3(mm)^3 size range.

It was decided to discontinue to use the CO_2 laser as a source of carbon vapor, because it was not convenient to obtain high enough power densities to give free jet vaporization; in the effusive vaporization region there are more convenient heating arrangements that do not impose geometric restrictions and window protection problems. A carbon arc source is being considered as a source of effusively vaporizing carbon vapor.

7. PLASMA-POLYMERIZED FILMS

7.1 Introduction

At the DARPA Contract Review in Boulder (May 1974), one of the needs that become obvious was that of hermetically sealing the optical system from the environment, i.e., preventing the optical components from coming in contact with water vapor and/or oxygen. This is especially true for coatings of germanium,

where the bulk film was shown to oxidize in time producing GeO_2. Since the Ge-O bonds absorb near 10 μm, oxidization destroys the applicability of germanium as an antireflective coating. In addition, most other films were shown to contain pinholes which would allow water vapor to reach the KCl substrate.

The suggestion was made that a plasma-polymerized organic film could be made to hermetically seal the optical component after the application of an antireflective coating. These films can be made thin enough to eliminate the effect of any absorptions in the infrared region of the spectrum. Since some early work at Penn State had developed the techniques for making these films (25-27), Dr. Stickley asked this group to prepare some of these films for evaluation.

It is significant to note that most other investigators in this field have used r.f. excitation as a means of producing species for the polymerization reactions. However, our approach has been to use microwaves for this purpose. The results appear to be rather different. We believe that the microwave excitation completely atomizes the reactant gas(es), whereas r.f. excitation only breaks some of the molecular bonds; thus, two rather different systems are polymerizing, giving rather different results.

7.2 Apparatus and Procedure

Figure 18 is a schematic diagram of the apparatus used in the preparation of the plasma-polymerized films. The microwave cavity excitation system consists of an Ophthos cylindrical cavity driven at a frequency of 2450 MHz by a Raytheon Diatherm unit. The reactor tube was constructed of 13 mm Vycor tubing; the substrate holder was made from Vycor rod and served to hold the substrates normal to the axis of the reactor tube. The substrates were 8 mm x 8 mm microscope slide cover slips made of a soda-lime-silicate glass which were cleaned with a detergent solution and then with distilled water in an ultrasonic cleaner, rinsed with acetone, trichloroethylene and methanol, and finally stored in methanol.

A substrate to be coated was placed in the reaction tube and the system evacuated to at least 10^{-5} torr. The reactant gas was then introduced at a pressure in the range of 3 to 7 torr and the system isolated. The microwave generator was set at the desired power level and a discharge initiated with a Tesla coil. Manual feedback kept the power constant throughout the run.

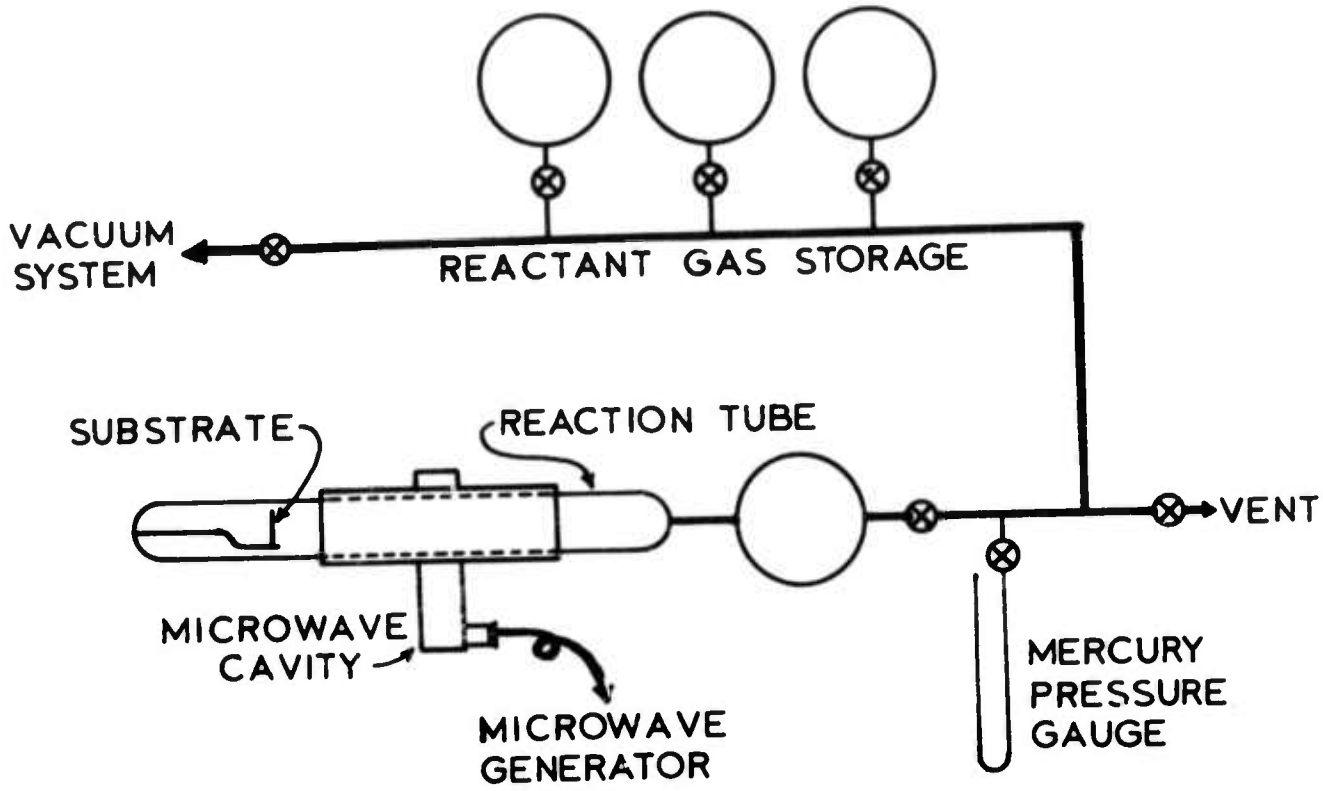

Figure 18. Schematic Diagram of the Microwave Plasma-Polymerization Apparatus.

In order to vary the hydrogen/carbon ratio in the reaction system, three different gases were used for the plasma-polymerization process: methane (CH_4), ehtylene (C_2H_2), and a mixture of ethylene and hydrogen. Films were produced under various deposition conditions. The variables were reactant gas pressure, system pressure, microwave power, time, and distance between the center of the plasma region and the substrate.

7.3 Results

The results of many different experimental runs are given in Table IV. The most critical factor in the production of uniform, hole-free films appeared to be the distance between the substrate and the center of the plasma. At 1 cm some of the films had a rough, lumpy surface, indicating that the films had experienced too high a temperature and had buckled. The films with the best appearance were prepared at a distance of 3 cm; deposition rates were too slow for distances greater than this.

Table IV

Plasma-Polymerized Films

Reactant Gas	H/C Ratio	Plasma-Substrate Distance (cm)	Total Pressure (torr)	Net Power (watts)	Time (min)	Avg. Thick-ness (Å)	Film* Color
CH_4	4.0	1.0	3.1	40	25	6600	LB
CH_4	4.0	1.0	3.15	40	15	4400	LB
CH_4	4.0	1.0	3.1	40	5	2500-6000	CL
CH_4	4.0	3.0	3.1	40	5	100	CL
CH_4	4.0	3.0	3.1	40	25	-	CL
CH_4	4.0	2.0	3.1	40	30	1200	LB
CH_4	4.0	2.0	3.1	60	30	1100	VLB
CH_4	4.0	3.0	3.1	40	30	380	CL+
CH_4	4.0	4.0	7.0	40	60	200	CL
CH_4	4.0	3.0	6.9	40	60	680	Milky
CH_4	4.0	3.0	3.0	40	60	750	CL+
C_2H_2	1.0	3.0	7.0	40	18	1100	VLB**
C_2H_2	1.0	3.0	3.1	10	4	100	CL
C_2H_2	1.0	1.0	7.0	20	4	17000	B**
C_2H_2-H_2	1.6	3.0	6.5	30	25	520	VLB+
C_2H_2-H_2	1.6	1.0	6.5	10	5	4700	LB**
C_2H_2-H_2	1.6	3.0	6.5	30	25	1200	VLB+

* LB = Light Brown VLB = Very Light Brown
CL = Clear B = Brown

** Film partially pyrolyzed

\+ Examined by electron diffraction and microscopy by Mr. Joseph Comer, AFCRL.

Several conclusions were drawn from the study of deposition parameters. The deposition rate is constant for a given distance and is independent of microwave power, pressure and time (for the range of conditions studied). Film thickness increases linearly with time (Figure 19), which is consistent with the observations of others (28,29). The deposition rate increases with decreasing H/C ratios in the starting reactant gas (also shown in Figure 19). Figure 20 shows the dependence of deposition rate on the distance of the substrate from the center of the plasma region. The rate is very low for distances greater than 4 cm, and the rate is very high for distances greater than 2 cm. However, the film is easily pyrolyzed by the microwave excitational forces at distances less than about 2 cm. Thus, 3 cm was chosen as an optimum distance for deposition studies. The film colors appear to be dependent on the amount of heating, i.e., the distance and the time of deposition, although no substrate temperatures were measured.

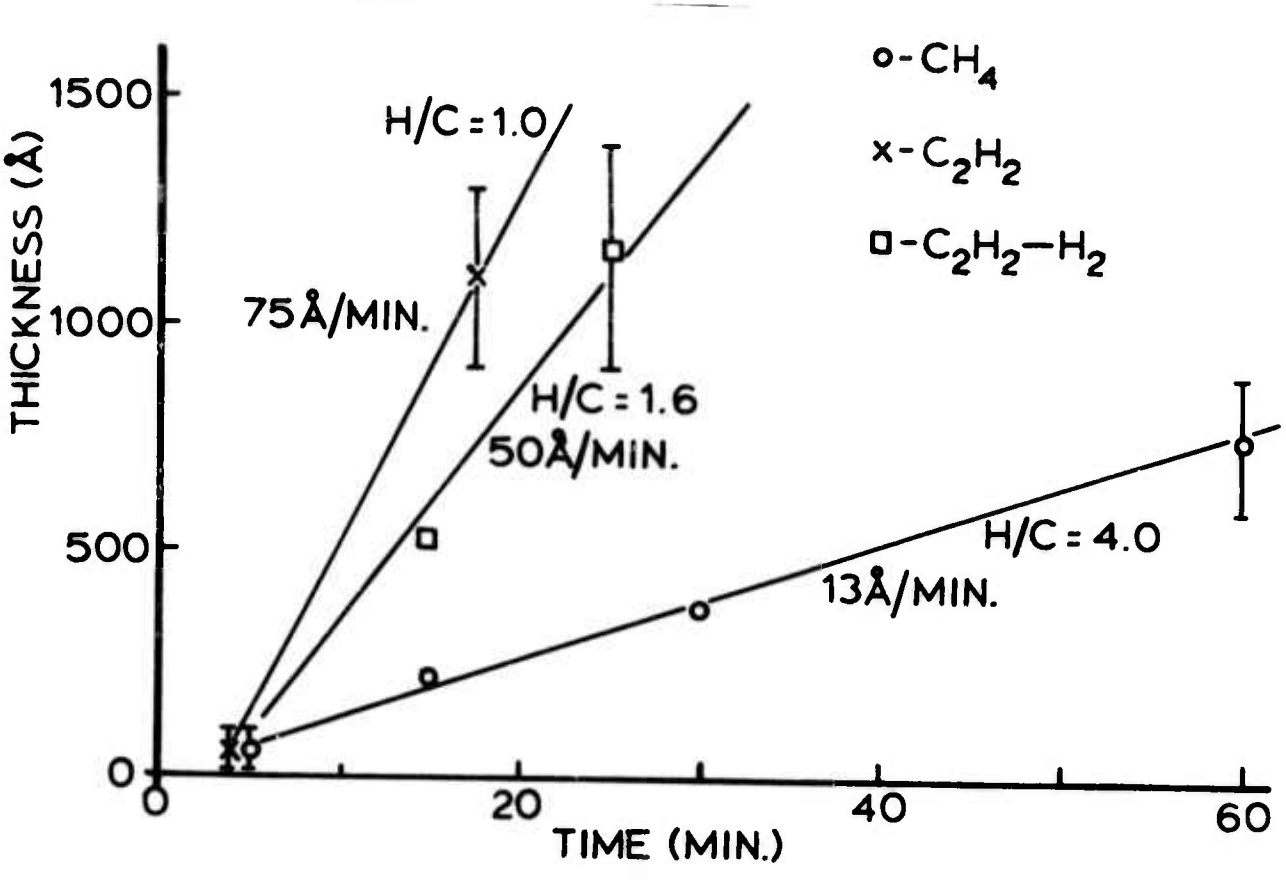

Figure 19. Deposition Rates for Films Prepared from Different Reactant Gases (plasma-substrate distance = 3 cm).

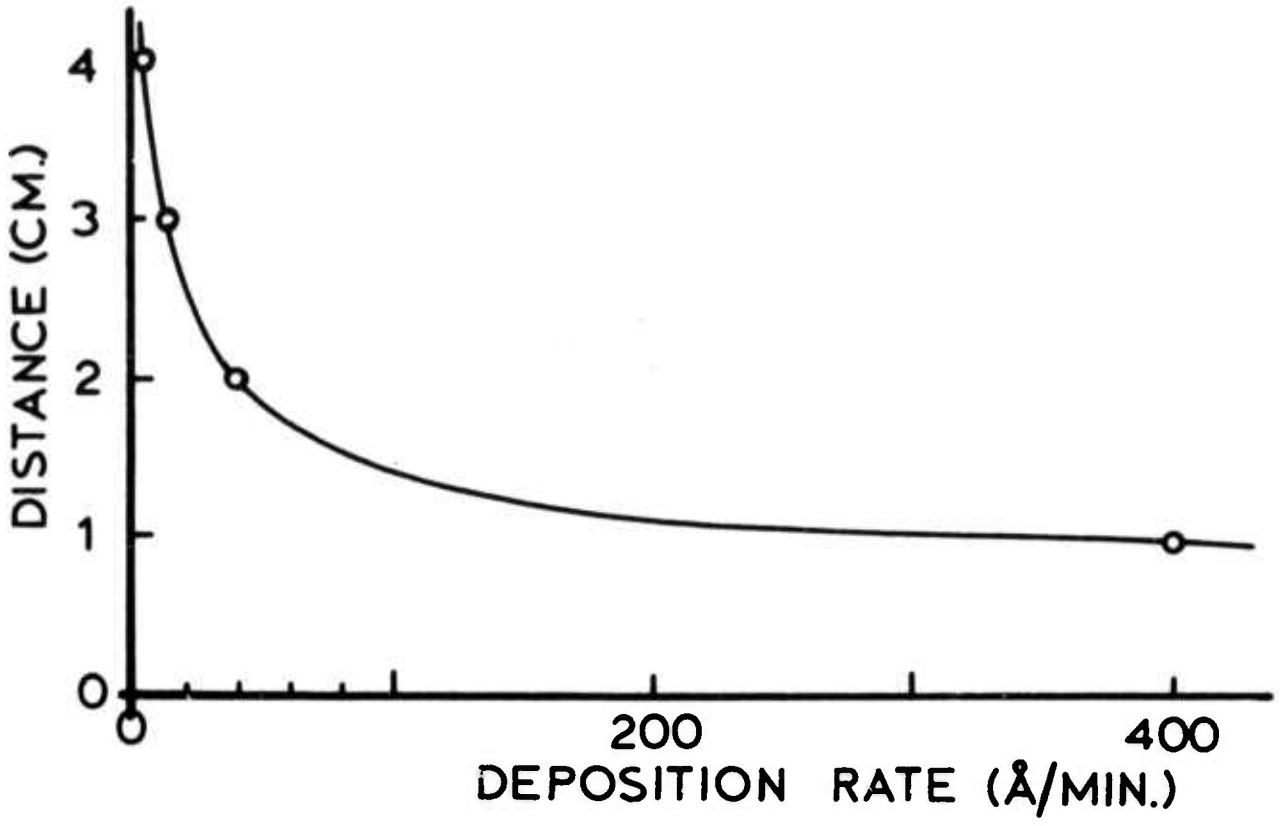

Figure 20. Deposition Rate vs. Plasma-substrate Distance for Films Prepared from Methane (H/C = 4).

7.4 Film Characterization

The films were examined both with an optical microscope and a scanning electron microscope. With the exception of those films which were pyrolyzed, the films were homogeneous and free of pinholes at magnifications up to 1000X.

Several samples (as marked in Table IV) were sent to Mr. Joseph Comer of AFCRL for electron microscopic examination. Two of the films, approximately 1000Å thick, appeared to be amorphous. Two other films which were much thinner (400-500Å) gave a transmission diffraction pattern indicative of a diamond cubic structure. Reexamination of these films by reflected electron diffraction showed a slight diffuse ring, indicating a crystallite size of <100Å, as well as a graphite 002 reflection. This data tends to support the 5-carbon tetrahedral building-block structure proposed by Vastola and Greco (26). TEM indicated a homogeneous film structure.

8. DURABILITY TESTING OF THIN FILMS

8.1 Introduction

The term "adhesion" usually means the ability of a film and substrate to remain in contact under a tensile force. Most tests of adhesion involve a very complicated mixture of shear and tensile stresses at the interfacial region. Failure of a film is often attributed to poor adhesion, when in reality it has been detached by high internal stress. Clearly, such a film is no more useful than a film with poor adhesion.

For coatings on laser windows, we are primarily interested in the "durability" of a film. Therefore, we have been interested in how one can test the durability of a film. To obtain a wide variety of durability, we have adopted a fourfold approach to its definition:

a) a scratch test of adhesion;

b) an abrasion test;

c) a stress evaluation; and

d) an examination of the film-substrate interface with ion scattering and Auger Electron Spectroscopy.

8.2 Scratch-Test

We have been using the "scratch" test which was used originally by Heavens (30) and developed further by Benjamin & Weaver (31,32). This method uses a smoothly rounded point which is drawn across the film surface. A vertical load is applied until the film is stripped from the surface. This load is a measure of the adhesion of the film. Figure 21 shows a diagram of the scratch tester. The instrument uses a tungsten carbide dial indicator contact point, 400 μm diameter, as a stylus. We have adopted this method because it is an inexpensive and rapid measure of adhesion. This test is useful in comparing the quality of films sputtered under different conditions and in evaluating the influence of substrate preparations on thin film adhesion. Table V shows the effect of various substrate preparations and sputtering conditions on "adhesion" by the "scratch" tester.

The "scratch" test has been criticized by Butler, et al; (33) specifically, the test is dependent on the hardness of the film and of the substrate, and optical methods of determining de-adherence are not reliable. It has been our experience that the de-adherence is easily detectable by placing a lamp below

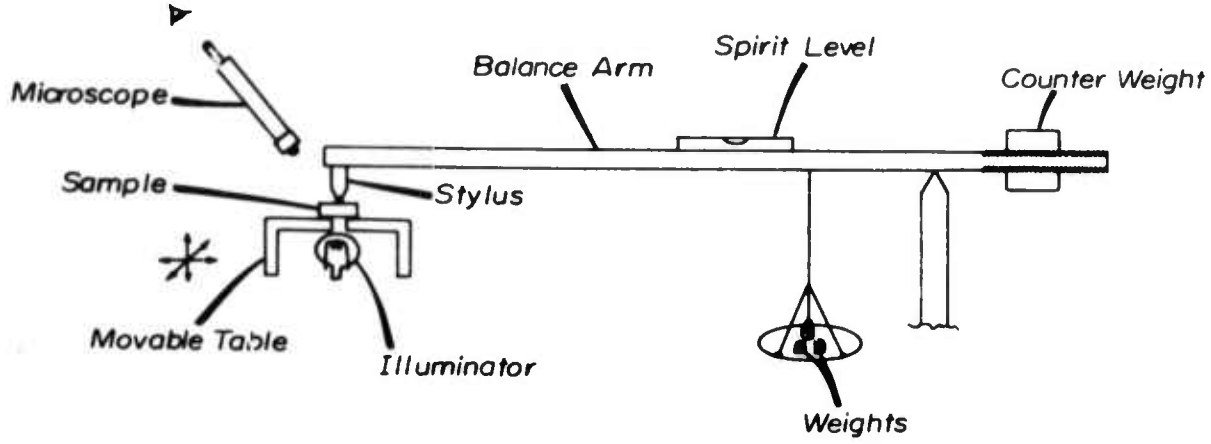

Figure 21. Schematic Diagram of "Scratch" Test Apparatus.

Table V

Adhesion of Germanium Films on Potassium Chloride Substrates

("Scratch Test Hardness" of KCl = 70 Grams)

Sputtering Conditions				Substrate Prep.*	Film Thickness (μm)	Adhesion "Scratch-Test" Value (grams)	"Adhesion (normalized to KCl)
R.F. Power (watts)	R.F. Voltage (volts)	Argon Pressure (mTorr)	Heat Transfer Agent				
25	390	30	None	a	2	25	.36
25	390	30	None	b	2	50	.71
25	390	30	None	c	2	95	1.4
25	390	30	None	d	1	180	2.6
25	390	30	None	d	2	180	2.6
25	380	30	Gallium	d	1	160	2.3
150	1060	20	Gallium	d	2	110	1.6
150	980	40	Gallium	d	2	150	2.1
200	1160	20	Gallium	d	2	130	1.9
100	920	20	Gallium	d	2	125	1.8
2x2 Glass Microscope Slide, 8x8 mm				e	-	>600	-

*Substrate preparation after cleaving:

a) No polishing; clean with ethyl ether after cutting.

b) Mechanical polishing with 25 μm alumina and methanol; chemical polishing with ethanol.

c) Water polishing; mechanical polishing with 25 μm alumina and methanol; chemical polishing with ethanol.

d) Mechanical polishing with 25 μm alumina and methanol; chemical polishing with solution of 2 parts glacial acetic acid, 1 part concentrated hydrochloric acid (2 minutes); ethanol rinse; ethyl ether rinse.

e) Cleaned with ethanol.

the transparent substrate and viewing the "scratch" from above with a 20X microscope.

In the original analysis of the "scratch" test technique, Benjamin & Weaver (31,32) proposed that the loosening of the film from a substrate was related to the deformation of the substrate by the stylus point. The substrate surface is plastically deformed; the film is also deformed to contour the shape of the indentation. This causes stretching of the film and a shearing force between the film and the substrate surface. With increased loads the shearing force increases until it reaches a value at which the adhesive bonds between the film and substrate are broken. If this is true, the objection of Butler et al., (33) with reference to the dependence of the test value on film and substrate hardness is valid. However, it need not limit the validity of the "scratch" testing techniques.

If the substrate deforms as described by Benjamin & Weaver (31,32) then film detachment is likely produced by the shearing force they describe. It is a simple task to determine if a given substrate deforms in the detachment of a given film. The measurement of the load necessary to produce a given track width on any substrate would indicate if the substrate is being deformed during film detachment. For example, the track width we observe in the detachment of a 1-2 μm germanium films on KCl substrates is 70 - 80 μm. A 70 gram vertical load will produce a track width of 70 - 80 μm on a KCl substrate without a film.

For a germanium film on a KCl substrate, a load of $\geq$ 70 grams will remove the film and deform the substrate, the actual load being a function of the adherence of the film. Conversely, a 10 μm germanium film on a glass substrate requires a vertical load of 520 grams for film removal, producing a track width of 110 μm. However, the glass substrate shows no track nor evidence of deformation at loads up to 600 grams. Thus, the mechanism of film removal for germanium on glass would be different from the removal of germanium on KCl.

Therefore, we recommend that measurements obtained from a "scratch" tester be reported as values normalized to the substrate. Thus, for a value of 180 grams for one germanium film on KCl, we would report such a value as $\frac{180}{70}$ or 2.6. If we compare this to a normalized value of 1.4 (corresponding to a 95 gram vertical load) for another germanium film on KCl, we immediately see that the former value indicates better adhesion. But we also see that since

both values are greater than one, the substrate was deformed and the mechanism of removal was probably the same in both cases.

8.3 Abrasion Test

The abrasion tester uses essentially the same apparatus as the "scratch" test. The stylus is replaced by a 1/4 inch diameter "Cratex" rubber tip impregnated with emery. The sample stage is rotated at 70 rpm beneath the "Cratex" tip at varying loads. This method is capable of sorting samples in order of durability to abrasion.

For germanium on KCl substrates we have arbitrarily adopted a procedure of subjecting the films to increasing vertical loads for 1 minute until a load is attained which results in complete film removal. Table II shows the abrasion results obtained for some germanium films on KCl.

Table VI

Abrasion Test Values for 2 μm Thick Germanium Films on KCl

Sputtering Conditions			
R.F. Power (watts)	Argon Pressure (mTorr)	Heat Transfer Agent	Vertical Load (grams)
150	15	Gallium	50
150	30	Gallium	150
25	30	None	100

8.4 Stress Testing

Two types of stress may occur in thin films: thermal stress, due to different thermal coefficients of the film and substrate, and a residual internal stress, called intrinsic stress. The stress may be either compressive (i.e., the film would like to expand) or tensile. In extreme cases, the film may buckly up on the substrate (compressive stress) or peel back from the substrate (tensile stress).

We have adopted two techniques of stress evaluation. Large stress will produce bowing of 8 x 8 x 0.1 mm glass substrates. Relative values of stress were obtained by measuring the center deflection of the glass substrate. Figure 2 (page 3) shows relative stress in germanium films as a function of sputtering parameters. From these plots we see that films with a compressive stress were formed at low gas pressure and high rf-power, while the opposite was true for films having a tensile stress.

For films deposited on KCl, we have adapted the technique used by Beams (34). In this test a hole is drilled through the KCl substrate with a water jet. If the stress is compressive the film will bow above the surface of the substrate, and the bulge deflection (δ), will be related to the stress by (34)

$$S_c = \frac{2}{3} \frac{E_f}{1 - \gamma} \frac{\delta^2}{r^2} \qquad (2)$$

where S_c = compressive stress (dynes/cm^2),

E_f = Young's modulus for the film (9.9×10^{11} dynes/cm^2 for germanium),

γ = Poisson's ratio for the film (0.27 for germanium) and

r = radius of the hole (cm).

For a germanium film this becomes,

$$S_c = 9.0 \times 10^{11} (\delta/r)^2 \qquad (3)$$

If the stress is tensile a pressure must be applied to produce the bulge deflection. For a germanium film the equation becomes:

$$p = \frac{4 d_f \delta}{r^2} [S_* + 9.0 \times 10^{11} (\delta/r^2] \qquad (4)$$

where p = the applied pressure (dynes/cm^2)

d_f = film thickness (cm), and

S_* = tensile stress (dynes/cm^2)

8.5 Examination of Film - Substrate Interface

The type of interface will determine the adhesion between the film and the substrate. Three types of interfaces may be considered: (35)

(a) In the monolayer-to-monolayer type of interface there is an abrupt change from the film material to the substrate in a distance on the order of atomic separations (2-5 Å).

(b) The diffusion interface arises from interdiffusion between film and substrate or from solubility of one or both materials in the other. Sputtering at high energy may produce a diffusion type of interface due to surface penetration by bombarding ions.

(c) The compound interface has an intermediate layer. The film and substrate are bonded together by forming compounds with each other or with a gas such as oxygen. Many metal films adhere to glass substrates in this way.

Ion scattering and Auger Electron Spectroscopy enable us to sputter through a deposited film and examine the species present in the interface. In this way we may evaluate the interfacial breadth and attempt to identify the type of interface. In addition, we may detect impurities which could be influencing adhesion. This work has not been completed; hence standard procedures cannot be recommended at this time.

9. DETERMINATION OF STRESS-OPTIC COEFFICIENT OF ZnSe AT 10.6 μm

At the request of the contract monitor and other scientists at the Air Force Cambridge Research Laboratories, the stress-optic coefficient of ZnSe was measured at 10.6 μm.

The determination of the stress-optic coefficient of polycrystalline ZnSe involves subjecting the specimen, in the form of a rectangular parallelpiped, to a unidirectional stress and measuring the birefringence produced by the stress. It can be shown that the birefringence produced by a stress σ (compression) is given by:

$$(\Delta n_{11} - \Delta n_{\perp}) = \frac{n^3}{2} (q_{11} - q_{12})\sigma \qquad (5)$$

where n is the refractive index of the material under normal conditions (i.e. under zero stress), σ the applied uniaxial stress, Δn_{11} and $\Delta n_{\perp}$ are respectively the changes in the refractive index of the material for light polarized with electric vector parallel and perpendicular to the direction of stress, and q_{11} and q_{12} are the piezo-optic coefficients. In the above relation the usual convention of treating the stress as positive when it is in tension and

negative under compression has been adopted. Equation (5) can also be written as

$$(\Delta n_{11} - \Delta n_{\perp}) = C_{\lambda}\sigma, \tag{6}$$

where $C_{\lambda} = \frac{n^3}{2}(q_{11} - q_{12})$ is the stress-optic coefficient.

Since the stress birefringence at 10.6 μm is expected to be small, the technique of using a Senarmont Compensator was employed in these studies. Figure 22 represents a schematic diagram of the experimental arrangement

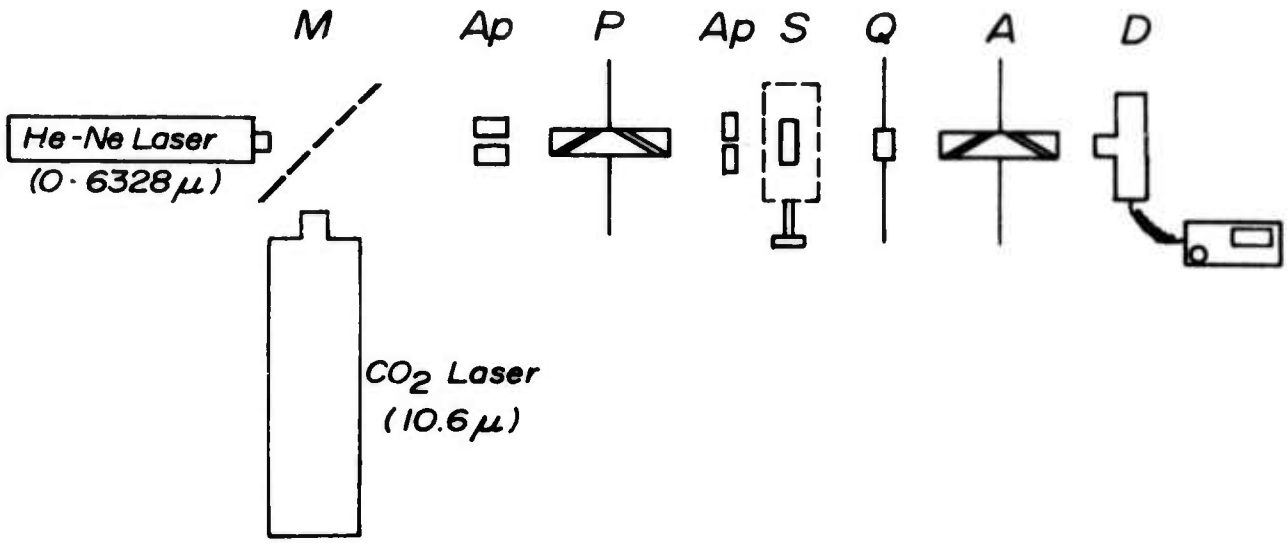

Figure 22. Schematic Diagram of the Experimental Arrangement for Measuring the Stress-Optic Coefficient at 10.6 μm.

used for measuring C_{λ} of ZnSe at 10.6 μm. The experimental sample, S, in the form of a rectangular parallelpiped was subjected to a compressional stress along its length with the help of a small Black-hawk press, whose end plattens were machined flat and true to be parallel. One important condition that must be satisfied to obtain reliable results from these measurements is that the stress distribution in the specimen must be uniform. This was achieved by making the length of the experimental specimen about three times the breadth and by confining the measurements to the middle region of the specimen. Furthermore, lead spacers were employed on both sides of the specimen as the medium for transmitting the stress from the compressing apparatus to the specimen.

The polarizer, P, and the analyzer, A, were made of ZnSe optical flats mounted at the Brewster angles corresponding to 10.6 μm, and the entire assemblies were mounted in suitable graduated circles capable of being read to one minute of arc. The quarter wave plate for λ 10.6 μm (made of CdS crystal) also was mounted in a similar graduate circle. Thus, since the polarizer, quarter wave plate, the experimental specimen and the analyzer were all transparent in the visible region of the spectrum, a He-Ne laser emitting λ = 6328 Å was employed initially to align the optical train before switching over to the 10.6 μm wavelength from a Coherent Radiation 50W CW/pulse CO_2 laser.

The detector was a Coherent Radiation thermopile power meter, whose lower limit of sensitivity was increased by about 20 times by modifying the detector circuit to produce a full scale deflection for 0.05 Watt power incident on it. With such a detector, fairly reproducible results could be obtained, and there was no need to incorporate a more sensitive TGS pyroelectric detector coupled to a PAR HR8 Lock-in Amplifier System, even though such a system was available.

The graphite apertures, A_p, helped align the optical train and also fix the region of the experimental sample under study. Once the optical system was aligned with the He-Ne laser beam, the mirror, M, was inserted before turning on the CO_2 laser system.

With such an arrangement, light polarized at 45° to the vertical was allowed to be incident on the experimental sample subjected to a vertical compressive stress. The quarter wave plate was also aligned such that its slow axis was at 45° to the vertical. The analyzer, which was set for extinction, will be at -45° to the vertical, when the isotropic experimental specimen is under no load (i.e. at the start of the experiment). When the specimen is subjected to a stress, the analyzer will have to be rotated through an angle, θ°, to maintain the extinction condition. It can be shown (36,37) that the relative phase retardation, δ, is given by

$$\delta = \frac{360t\ (\Delta n_{11} - \Delta n_{\perp})}{\lambda} = 2\theta, \qquad (7)$$

where t is the thickness of the specimen and λ the wavelength of light employed. The sign of rotation of the analyzer (clockwise or counterclockwise) determines

the sign of θ, and hence the sign of $(\Delta n_{11} - \Delta n_{\perp})$, from Equation (7), and hence the value of C_λ with the help of Equation (6). Thus a measurement of θ yields the value of $(\Delta n_{11} - \Delta n_{\perp})$.

Using this experimental arrangement the values of C_λ of ZnSe at 10.6 μm was found from the average of nine measurements to be -11.9_2 Brewsters. This compares favorably with the value -13.1 Brewsters obtained by Professor Corelli (38) of Rensselaer Polytechnic Institute on a similar sample of ZnSe. Using this value the various other piezo-optic and strain-optic coefficients were evaluated with the help of the elastic constants data. The elastic constants of polycrystalline ZnSe were computed from the elastic constants values of single crystalline ZnSe as reported by Lee (39), making use of Hill's technique (40) of averaging Voight's and Reuss' averages. The pertinent values for ZnSe are given as follows:

Elastic Constants of Single Crystalline ZnSe (39):

$C_{11} = 8.59 \times 10^{11}$ dynes/cm^2
$C_{12} = 5.06 \times 10^{11}$ dynes/cm^2
$C_{44} = 4.06 \times 10^{11}$ dynes/cm^2

Polycrystalline ZnSe:

Bulk Modulus $K = 1/3\ (C_{11} + 2C_{12}) = 6.24 \times 10^{11}$ dynes/cm^2
Shear Modulus $G = 1/2\ (C_{11} - C_{12}) = 2.91 \times 10^{11}$ dynes/cm^2

At 10.6 μm:

Stress-optic coefficient C = -11.9 Brewsters
Piezo-optic coefficient $(q_{11} - q_{12}) = -1.71 \times 10^{-13}$ cm^2/dyne
Strain-optic coefficient $(p_{11} - p_{12}) = -0.100$

10. REFERENCES

1. Loomis, J. S., Technical Report No. AFWL-TR-72-180, January 1973.
2. Messier, R., Ph.D. Thesis, The Pennsylvania State University, 1973.
3. Pastor, R. D., and Braunstein, M., Tech. Rept. No. AFWL-TR-72-152, Vol. II, Air Force Weapons Lab., Kirtland Air Force Base, New Mexico, July 1973.
4. Burge, D. K., and Bennett, H. E., J. Opt. Soc. Am. 54, 1428 (1964).
5. Archer, R. J., J. Phys. Chem. Solids 26, 343 (1965).
6. Vedam, K., and So, S. S., Surf. Sci. 29, 379 (1972).
7. Ohlidal, I., and Lukes, F., Opt. Acta 19, 817 (1972).
8. Nadeau, J. S., J. Appl. Phys. 34, 2248 (1963).
9. Green, M., Kafalas, J. A., Robinson, P.H., in "Semiconductor Surface Physics," University of Pennsylvania Press, Philadelphia, Pa., 1957, p. 349.
10. Bauer, R. S., and Galeener, F. L., Solid State Commun. 10, 1171 (1972).
11. Helms, C. R., Spicer, W. E., and Pereskokov, V., Appl. Phys. Lett. 24, 318 (1974).
12. Ligenza, J. R., J. Phys. Chem. 64, 1017 (1960).
13. Neuberger, M., Electronic Prop. Inf. Cent., Culver City, Ca., Data Sheet No. DS-157 (1967).
14. Vaughn, D. A., in "Standard X-ray Diffraction Powder Patterns," Nat. Bur. Stds. Monograph 25, Section 3, H. E. Sawson, M. C. Morris, E. H. Evans, and L. Ulmer, eds., Washington, D. C., 1964, p. 21.
15. Scherrer, P., Göttinger Nachrichten 2, 98 (1918).
16. Rau, R. C., "Routine Crystallite-size Determination by X-ray Diffraction Line Broadening," in Advances in X-ray Analysis, Vol. 5, W. M. Mueller, ed., Plenum Press, New York, 1962, p. 104.
17. Semiletov, S. A., Sov. Phys. Cryst. 1, 236 (1956) [English translation].
18. Rumsh, M. A., Novik, F. T., and Zimkina, T. M., Sov. Phys. Cryst. 7, 711 (1963).
19. Shiroji, M., and Suito, E., Jap. J. Appl. Phys. 3, 314 (1964).
20. Colby, J. W., "Quantitative Microprobe Analysis of Thin Insulating Films," in Advances in X-ray Analysis, Vol. 11, J. B. Newkirk, G. R. Mallett, and H. G. Pfeiffer, eds., Plenum Press, New York, 1968, p. 287.

21. "Selected Values of Chemical Thermodynamic Properties," NBS Technical Note, 270-3 (1968).
22. Aisenberg, S. and Chabot, R., J. Vac. Sci. Tech. 8, 112A (1971).
23. Fedosev, D. V., Galimov, E. M., Varnin, V. P., Prokhorov, V. S., and Deryagin, V., Zh. ETF Pis. Red. 14, 80 (1971).
24. Angus, J. C., Will, H. A., and Stanko, W. S., J. Appl. Phys. 39, 2915 (1968).
25. Vastola, F. J., and Wightman, J. P., J. Appl. Chem. 14, 69 (1964).
26. Vastola, F. J., and Greco, B., unpublished research, The Pennsylvania State University.
27. Greco, B., M.S. Thesis, The Pennsylvania State University, 1964.
28. Mearns, A. M., Thin Solid Films 3, 210 (1969).
29. Yasuba, Y., and Lamaze, C. E., J. Appl. Polym. Sci. 15, 2281 (1971).
30. Heavens, O. S., J. Phys. Radium 11, 355 (1950).
31. Benjamin, P., and Weaver, C., Proc. Roy. Soc. London, A254, 177 (1960).
32. Benjamin, P., and Weaver, C., Proc. Roy. Soc. London, A274, 267 (1963).
33. Butler, D. W., Stoddart, C. T. H., and Stuart, P. R., J. Phys. D. 3, 877 (1970).
34. Beams, J. W., in "Structure and Properties of Thin Films", C. A. Neugebauer, J. B. Newkirk, and D. A. Vermilyea (eds.), John Wiley & Sons, Inc., New York, 1959, p. 183.
35. Chapman, B. N., J. Vac. Sci. Technol. 11, 106 (1974).
36. Hartshorn, N. H., and Stuart, A., "Crystals and the Polarizing Microscope," 4th ed., Edward Arnold Publishers, London, 1970, pp. 309-310.
37. Born, M., "Principles of Optics," Pergamon Press, 4th ed., 1970, pp. 24-32.
38. Corelli, J. C., private communication through Major Charles Collins, AFCRL, 1974.
39. Lee, J., Appl. Phys., 41, 2988 (1970).
40. Hill, R., Proc. Phys. Soc. (London) 65A, 349 (1952); O. L. Anderson, in "Physical Acoustics", Vol. 3B, Academic Press, New York, 1965, Chapt. 2.